AD-A131 173 NEUTRAL FLOW THROUGH ION CLOUDS(U) BERKELEY RESEARCH 1/1
ASSOCIATES INC CA C W PRETTIE 01 DEC 82 PD-BRA-82-282R
DNA-TR-81-212 DNA001-81-C-0061

UNCLASSIFIED F/G 18/3 NL

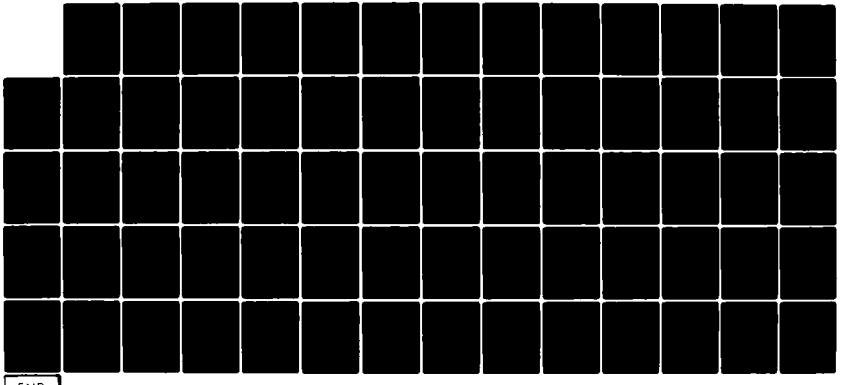

END
DATE FILMED
9 83
DTIC

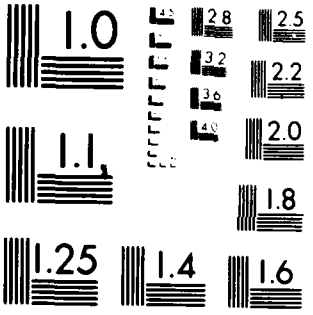

DNA TR-81-212

NEUTRAL FLOW THROUGH ION CLOUDS

Clifford W. Prettie
Berkeley Research Associates, Inc
P.O. Box 983
Berkeley, California 94701

1 December 1982

Technical Report

CONTRACT No. DNA 001-81-C-0061

THIS WORK WAS SPONSORED BY THE DEFENSE NUCLEAR AGENCY
UNDER RDT&E RMSS CODE B322082466 S99QAXHC00054 H2590D.

Prepared for
Director
DEFENSE NUCLEAR AGENCY
Washington, DC 20305

UNCLASSIFIED

SECURITY CLASSIFICATION OF THIS PAGE (When Data Entered)

REPORT DOCUMENTATION PAGE		READ INSTRUCTIONS BEFORE COMPLETING FORM
1. REPORT NUMBER DNA TR-81-212	2. GOVT ACCESSION NO. AD-A131 173	3. RECIPIENT'S CATALOG NUMBER
4. TITLE (and Subtitle) NEUTRAL FLOW THROUGH ION CLOUDS		5. TYPE OF REPORT & PERIOD COVERED Technical Report
		6. PERFORMING ORG. REPORT NUMBER PD-BRA-82-282R
7. AUTHOR(s) Clifford w. Prettie		8. CONTRACT OR GRANT NUMBER(s) DNA 001-81-C-0061
9. PERFORMING ORGANIZATION NAME AND ADDRESS Berkeley Research Associates, Inc. P.O. Box 983 Berkeley, California 94701		10. PROGRAM ELEMENT, PROJECT, TASK AREA & WORK UNIT NUMBERS Task S99QAXHC-00054
11. CONTROLLING OFFICE NAME AND ADDRESS Director Defense Nuclear Agency Washington, D.C. 20305		12. REPORT DATE 1 December 1982
		13. NUMBER OF PAGES 68
14. MONITORING AGENCY NAME & ADDRESS(if different from Controlling Office)		15. SECURITY CLASS (of this report) UNCLASSIFIED
		15a. DECLASSIFICATION/DOWNGRADING SCHEDULE N/A

16. DISTRIBUTION STATEMENT (of this Report)

Approved for public release; distribution unlimited.

17. DISTRIBUTION STATEMENT (of the abstract entered in Block 20, if different from Report)

18. SUPPLEMENTARY NOTES

This work was sponsored by the Defense Nuclear Agency under RDT&E RMSS Code B322082466 S99QAXHC00054 H2590D.

19. KEY WORDS (Continue on reverse side if necessary and identify by block number)

Striations	Viscosity
Structure	PLACES
Barium Clouds	Ion-Neutral Coupled Flow
Neutral Flow	HANE

20. ABSTRACT (Continue on reverse side if necessary and identify by block number)

Ionospheric plasma clouds exert a drag force on the neutrals flowing through them which is generally neglected in plasma evolution analyses. This drag force can be significant in barium clouds and in late time HANE plasmas. The interaction between these two flows and its influence on plasma evolution and structuring are considered and presented in this report.

Based on momentum considerations alone the neutral slip speed past barium ions is reduced by 1 meter per second for every 1.7×10^{15} ions per

DD FORM 1 JAN 73 1473 EDITION OF 1 NOV 65 IS OBSOLETE

UNCLASSIFIED

SECURITY CLASSIFICATION OF THIS PAGE (When Data Entered)

20. ABSTRACT (Continued)

meter squared it passes through. This significant deceleration may be considerably reduced in small or high altitude barium clouds by viscous forces; however, in may cases ion clouds produce a wake in the neutral flow.

The wake of the neutral wind passing through barium clouds affects its evolution according to the cloud size, altitude, and peak ion density. The interaction between ions and neutrals may explain morphological differences between the evolution of large SPRUCE-, ESTHER- and IRIS-like clouds and small Avefria Dos-like ion clouds. The results of numerical simulations of these two different types of clouds with coupled ion-neutral flow are presented which show a tendency for the large cloud to bifurcate.

The possibility that ion-neutral interaction creates neutral turbulence which in turn leads to plasma structuring is also investigated.

PREFACE

The author would like to acknowledge the efforts of Dr. S.Y. Frank Chu who was responsible for the numerical simulation work presented in Section 3 and the efforts of John R. Ferrante who assisted in the development of the neutral flow algorithms. The author has benefited from interactions with Dr. Lewis M. Linson of SAI, Major Leon A. Wittwer of DNA and Dr. Joseph B. Workman of BRA.

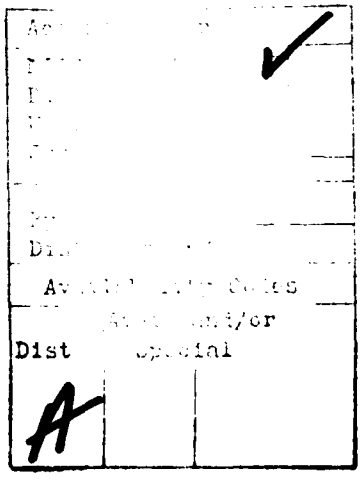

TABLE OF CONTENTS

LIST OF ILLUSTRATIONS

SECTION 1

INTRODUCTION

The purpose of this report is to bring to light an often overlooked physical effect that may be a factor in the evolution of electrostatic plasmas. This effect can alter their morphological evolution and may also be related to if not responsible for their structuring.

Most electrostatic analyses and simulations of plasma clouds assume that the coupling between the neutrals and ions is basically one-way. They account for the influence of neutral motion on ion motion but neglect how the reaction forces alter the flow fields of the neutrals.

As shown in Section 2 of this report, indeed, these reaction forces are significant and can alter the evolution of the plasma. Further, turbulence associated with these forces may be the cause of ion cloud structuring. These effects are of direct relevance to both HANE plasmas as well as barium plasma clouds.

In Section 3 of this report the results of numerical simulations which attempt to model the influence of the ions on the neutrals as well as the influence of the neutrals on the ions is presented. Two different plasma cloud cases are considered. One case demonstrates the effects of weak coupling parameters similar to those believed to characterize the barium cloud release Avefria Dos. The other case attempts to demonstrate more significant coupling with parameters similar to the ESTHER release of STRESS. McDonald et al.,(1979) notes that there are distinct large scale morphological differences between these two barium clouds and presents one explanation of

these differences. The results of the numerical simulations discussed in Section 3 suggest that coupling between ions and neutrals may be an additional source for these differences.

Conclusions of the report are presented in Section 4.

SECTION 2

COUPLED ION-NEUTRAL FLOW CONSIDERATIONS

2.1 MOMENTUM TRANSFER

The force equation for ions embedded in a neutral gas under the influence of electromagnetic forces is given by

$$m_i N_i \frac{du}{dt} = eN_i(E + u \times B) + \frac{N_i(v - u)e}{\mu}$$

where u, N_i, m_i and μ are the ion velocity, particle density, particle mass, and particle mobility in the neutral gas; where e, E, and B are the charge per particle, electric field vector and magnetic field vector, respectively; and where v is the neutral gas velocity. The second term on the right-hand side of the equation represents the forces that the neutral wind exerts on plasma clouds and the momentum transfer from the neutral gas to the ions.

Since momentum is conserved the momentum gained by the ions must represent a loss in momentum by the neutrals. The force equation for the neutrals with this reaction term is thus

$$mN \frac{dv}{dt} = -\nabla p + mN\nu\nabla^2 v + \frac{N_i(u - v)e}{\mu}$$

where N, m, p, and ν are the neutral density, neutral particle mass, pressure, and kinematic viscosity, respectively. This equation is the Navier-Stokes equation with the inclusion of the ion drag force.

Of significant interest is the magnitude of the ion drag term. The absolute value of the drag deceleration

can be obtained by dividing the neutral force equation by mN giving

$$\frac{dv}{dt} = - \frac{\nabla p}{mN} + \nu \nabla^2 v + \frac{N_i e}{mN \mu} (u - v)$$

and focussing attention on the last term on the right-hand side of the equation. This term is essentially the product of a mass density ratio between the ions and neutrals, the slip velocity, and the collision frequency (defined by $e/\mu m_i$).

For practical purposes it is easier to consider the form presented above because $e/mN\mu$ can be treated as roughly constant with altitude. From McDaniel (1964, p. 725) the ionic mobility is given by

$$\mu = \frac{.505}{\sqrt{(k-1)\ mN}} \left(\frac{m + m_i}{m_i} \right)^{1/2}$$

where k is the dielectric constant of the neutral gas. The term $k-1$ should be closely proportional to neutral particle density especially at ionospheric particle density levels and the mobility consequently takes the form

$$\mu = \frac{A}{N} \left(\frac{m + m_i}{m\ m_i} \right)^{1/2}$$

where A is independent of density and particle mass. The dependence of μ on $1/N$ makes the denominator of the ion drag term independent of neutral particle density. While μ and N are strongly dependent upon altitude the only altitude dependence of the drag coefficient $e/mN\mu$ is due to the slowly changing effective particle mass and particle polarization of the air mixture.

The coefficient $e/mN\mu$ for barium ions can be evaluated from published laboratory measurements of the mobility of 2.25×10^{-4} m^2/volt-sec for barium in N_2 at 1 atm at 20°C (Brown, 1959, p. 62). With mN as 1.23 kgm/m^3 (Knapp and Schwartz, 1975, p. 8-2) at 20°C at 1 atm

$$e/mN\mu = 5.78 \times 10^{-16} \quad m^3/sec$$

The significance of the value of $e/Nm\mu$ can be seen by considering stationary ions and by neglecting all other neutral wind forces. Integrating the Navier-Stokes equation in time gives

$$\int \frac{dv}{dt}\, dt = -\int \frac{e}{\mu mN}\, N_i\, v dt$$

or

$$\Delta v = -\frac{e}{\mu mN}\, N_{Ti}$$

where Δv is the change in velocity of a neutral fluid particle passing through a cloud of ions with integrated content of N_{Ti}. Thus $e/Nm\mu$ is the change in neutral velocity per unit of integrated plasma ion content. For barium the neutral wind velocity is thus decreased by 1 m/sec for every 1.73×10^{15} ions per meter squared it passes through if the pressure and viscous forces are negligible.

For small barium clouds, such as Avefria Dos, the peak integrated content that the wind passes through may be only 3×10^{16} el/m^2 (10^7 el/cc over a 1 km e-fold radius) producing only a 10 m/sec change in the neutral wind speed. If the ion-neutral slip speed is high, say 60 m/sec, a 10 m/sec change in wind speed may not produce

a noticeable difference in evolution from the case of no drag effects. For larger clouds (48 kgm at 180 km) the peak field line integrated TEC can be as large as 2.4×10^{17} el/m^2 (Linson and Baxter, 1977) at early time. At early time in the barium cloud development these large values of TEC can exist in the dimension transverse to the wind. Changes in the wind velocity as large as 130 meters per second are predicted (if other forces are ignored) which should significantly affect the ion cloud evolution.

2.2 NEUTRAL FLOW CONSIDERATIONS

The problem of the flow of ionospheric neutrals through a cloud of ions fixed to field lines is analogous to the flow of a gas through a porous medium such as a sponge. While there is no analytical solution to this problem the analogy proves to be useful when considering the properties of the neutral flow to be expected.

To first order the neutral flow is reduced in proportion to the total ion content passed through. This first order solution would result from a balance between the fluid momentum term and the drag term in the Navier-Stokes equation with other terms ignored. The neutral flow resulting from this type of solution however is not divergenceless. Consequently, the density is enhanced and reduced in different regions of the ion cloud and pressure effects start to influence the flow. The pressure effects cause the flow to be diverted around the ion cloud and to be pulled back into the wake.

A significant force in the higher altitude neutral atmosphere is viscosity. Viscosity tends to smooth the flow pattern resulting from the pressure and drag forces. While the flow pattern remains similar in form, the magnitude of the decrease in the neutral velocity in the ion cloud wake is reduced by viscous forces. Viscous forces thus tend to de-emphasize the effects that ion drag has on plasma cloud evolution, especially as the cloud altitude is increased.

Perhaps one of the more exciting facets of ion neutral coupling effects is that neutral turbulence may be created. One would expect the flow through a porous obstacle to be turbulent especially on the wake side of the obstacle. Note that this side of the ion cloud is the side that typically forms structures suggesting that neutral turbulence could be the source of ion cloud structure. Further evidence for this suggestion is that the size of the eddies in the neutral flow roughly corresponds to the sizes of the ion cloud structures observed. The neutral turbulence structuring mechanism offers an alternative to the mechanism discussed by McDonald et al. (1981) to explain structure growth and size stabilization.

The inferences about the possibility of turbulence and the size of their eddies are made from Reynolds number considerations. Basically the size at which the viscosity terms in the Navier-Stokes equations are equal to the momentum terms of the equation can be used as a smallest eddy size (Landau and Lifshitz, 1959, p. 122) with an adjustment of $R^{1/4}$ to the slip velocity where R is the Reynolds number for the entire cloud. The momentum terms can be approximated to be of magnitude

$$\frac{v\ \Delta v}{L}$$

where L is the size of the structure, v is the slip speed through it, and v is the change in slip speed. The viscosity term can be similarly estimated to be

$$\nu\ \frac{\Delta v}{L^2}$$

where ν is the kinematic viscosity. The two terms balance when the Reynolds number for the flow through the feature is 1, i.e., when,

$$\frac{vL}{\nu} = 1$$

By assuming an arbitrary ion neutral slip speed of 100 meters per second through the entire cloud the eddy size can be given in terms of the kinematic viscosity. The kinematic viscosity is a strong function of altitude and, consequently, so is the eddy size. The eddy size for a range of altitudes is presented in Table 1.

The $R^{1/4}$ correction to the eddy size has been made with the assumption that the overall plasma cloud size is 5 kilometers. Essentially this correction term arises because the effective flow speed differential Δv, through the eddy region is somewhat less than the expected flow speed differential through the total cloud.

The proposed mechanism for creating structure has many desirable features in that it does not rely upon seed structure in the ionosphere to produce growth as does the gradient drift (Linson and Workman, 1970) instability. It does have its drawbacks, however, which

Table 1. Turbulent eddy size for various altitudes

Altitude (km)	Density[1] (kgm/m^3)	Temperature (°K)	Dynamic[2] viscosity (kgm/m-sec)	Kinematic viscosity (m^2/sec)	Eddy size (meters)	$R^{1/4}$ correction to 5 km cloud	Eddy size with correction (in meters)
120	2.49×10^{-8}	355	1.97×10^{-5}	7.91×10^{2}	7.91	5.01	40.0
140	4.05×10^{-9}	573	2.9×10^{-5}	7.16×10^{3}	71.6	2.89	207
160	1.28×10^{-9}	721	3.37×10^{-5}	2.63×10^{4}	263	2.09	548
180	5.28×10^{-10}	839	3.74×10^{-5}	7.08×10^{4}	708	1.63	1154
200	2.56×10^{-10}	933	4.01×10^{-5}	1.566×10^{5}	1566	1.34	2090

1. Knapp and Schwartz, 1975, p. 8-4

2. Weast, Astle, 1980, p. F-13

should be pointed out. One drawback is that the Reynolds number required to establish turbulence may be too large. Landau and Lifshitz (1959, p. 105) mention that for the case of a solid cylinder the Reynolds number required for the flow to become turbulent is 34. For the case of the ion drag effect perhaps such a large Reynolds number is not required because of the porous nature of the flow but in any event the required Reynolds number should probably be greater than ten. Apparently, for clouds less than 5 kilometers in extent the ions must be at an altitude less than 160 kilometers to produce turbulence.

Another drawback to note is that the eddy sizes predicted, though close to the sizes of barium structures, are nevertheless somewhat large especially for the higher altitude clouds. For many clouds the slip velocity is closer to 25 meters per second in which case the uncorrected eddy sizes increase by a factor of 4.

The high kinematic viscosity in the 180 to 200 kilometer altitude regime makes structuring by neutral turbulence to the scale sizes observed in barium releases difficult. It may be the case, however, that electrical coupling to lower (130 kilometer) altitude turbulence could play a role in setting structure sizes. This thought leads to still another structuring mechanism. Perhaps barium structure is created by neutral turbulence, either pre-existing or stimulated by images, in the 130 kilometer altitude regime which is coupled electrostatically to the barium cloud along field lines. The 100 meter size eddies predicted in this regime from viscosity considerations are in good agreement with observed striation sizes.

In summary, the neutral flow through a plasma cloud is similar to the flow of a gas through a porous medium.

Because the Reynolds number for the flow can be large, the neutral flow produced may be turbulent. Neutral turbulence is more likely at lower altitudes where the kinematic viscosity is less and probably difficult to produce above 200 kilometers. Turbulence in the neutral flow could conceivably be an alternative source of electrostatic plasma cloud structuring.

2.3 FIRST ORDER INFLUENCE OF ION DRAG EFFECTS ON PLASMA CLOUD MOTION

Neutral flow through ionospheric plasma creates an electrical current, J_w, carried by ions with value specified by

$$J_w = \frac{eN_i\ (\mu B)}{1 + (\mu B)^2}\ v \times i_z + \frac{eN_i}{1 + (\mu B)^2}\ v$$

If the current is divergenceless it will not produce motion in the plasma other than that required of the ions to carry the current. On the other hand if the current is not divergenceless electrical fields will be created to bleed off charge build-up. These electric fields become the source of plasma motion.

Divergent wind currents in plasma clouds are typically created by variations in the plasma density. Divergent wind currents can also be produced by variations in the neutral wind transverse to the geomagnetic field even though the plasma density is constant. While the divergence of the neutral wind is typically close to zero, the neutral wind current depends most strongly upon $\nabla \cdot v \times i_z$ which is typically not zero in ion drag flows.

Ion clouds which produce deceleration of the neutral flow can stimulate both of these two different sources of divergent wind currents--a situation which leads to interesting plasma flow properties. Consider the neutral flow through an ion cloud with a Gaussian spatial density distribution. To first order the neutral flow in the wake is linearly related to the integrated ion content that the neutrals pass through. Neglecting pressure and viscosity effects the idealized flow is as shown in Figure 2-1. The flow in this figure is always directed toward the right, only its magnitude in this direction changes. In the interior region of the plasma cloud the flow is not divergenceless and hence its pattern is somewhat unrealistic. In the wake region however the flow is divergenceless and, thus, potentially realistic.

The divergence of the wind driven component of the current is proportional to

$$\frac{\partial}{\partial y} N v_x$$

for the case where the magnetic field is into the paper and where μB has been assumed to be large. The regions of charge accumulation for this situation are schematically shown in Figure 2-2. In addition to the customary charge accumulation at the top and bottom of the ion cloud is a charge accumulation associated with the wake of the cloud.

The plasma flow associated with the customary charge accumulation is such that the ion cloud is moved toward the right along the centerline of the cloud. The flow associated with the wake, on the other hand, is directed toward the left along the wake centerline. Background

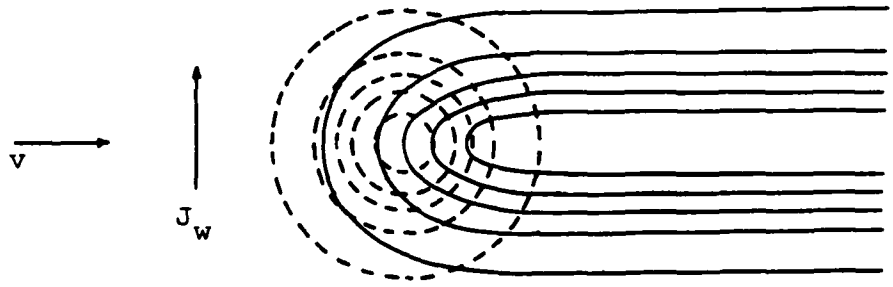

Figure 2-1. Idealized neutral flow through ion cloud. Dotted lines represent iso-density contours of the ion cloud and solid lines represent iso-speed contours of the x-directed neutral wind.

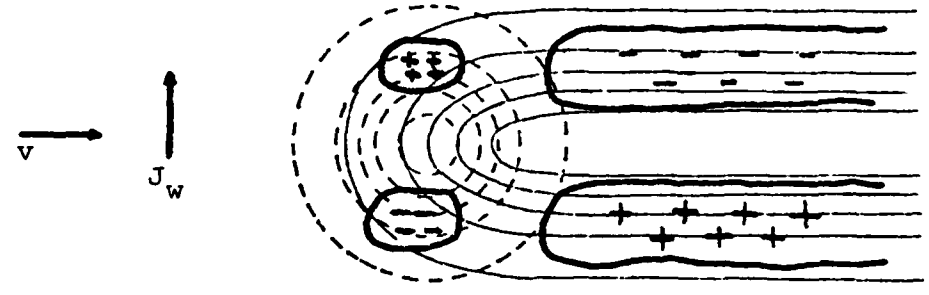

Figure 2-2. Regions of charge accumulation created by divergences in the wind current shown superimposed on flow and density contours.

plasma in the wake is, thus, directed toward the center of the barium cloud. This flow is somewhat unusual in that plasma is moving toward the left in response to winds toward the right. This phenomenon occurs bascially because the plasma is trying to maintain a constant ion-neutral slip speed in order to maintain a constant y-directed current.

One consequence of the mixture of the two different types of flow is that a dimple at the front of the ion cloud can be produced if the counter directed wake flow is strong enough. The plasma motion toward the right at the top and bottom of the cloud may become faster than at the centerline and as a result the cloud may be deformed until it begins to bifurcate. This type of behavior has not been reproduced in simulations which do not include ion-neutral coupling and is certainly of interest for understanding structuring processes in plasma clouds. Its effect is apparent in one of the simulations which follow.

SECTION 3

COUPLED ION-NEUTRAL FLOW NUMERICAL SIMULATION

3.1 COUPLED ION-NEUTRAL FLOW RELATIONS

In the following section results of simulations of the evolution of plasma clouds which include ion-neutral coupling effects are presented. In the simulations the ion drag effects on the neutral flow are included. This section presents the relations, the assumptions, and the approximations used for the simulation calculations.

Five relations are used in the calculations which involve five different quantities, namely, the neutral density, N, the plasma density, N_i, the flow potential, ϕ, and the x- and y-components of the neutral wind v.

The relations solved to find the ion behavior are the same as those conventionally used in 2-dimensional electrostatic plasma evolution simulations. A split step scheme is used. The plasma flow field is solved in the potential solving step from the specified values of plasma density and neutral wind. The flow is then used to update the plasma density values in the plasma convection step. The plasma convection step numerically advances the plasma density by using the continuity relation

$$\frac{\partial N_i}{\partial t} = -\nabla \cdot N_i \, \nabla\phi \times i_z$$

Note that the plasma flow velocity u is assumed to be incompressible and ϕ is the potential function describing this flow:

$$u = \nabla\phi \times i_z$$

The potential solving step solves the potential equation which specifies that the divergence of the total current be zero. For the simulations performed the Hall terms are assumed to be negligible. This assumption is frequently called the F-layer assumption and it implies the following relation for the potential:

$$\nabla \cdot N_i \nabla\phi = -\nabla \cdot N_i \mathbf{v} \times i_z$$

In this relation the neutral wind N_i and v are assumed known and ϕ is solved for using matrix inversion techniques.

Once N_i and ϕ are known the effect of ion drag on the neutral flow can be calculated. The neutral density and flow are also advanced through time using a split step technique. Given a known neutral flow velocity the neutral density is advanced in time using the continuity equation

$$\frac{\partial N}{\partial t} = -\nabla \cdot Nv$$

The neutral density flow is updated through time using the Navier-Stokes equation with an isothermal ideal gas approximation to the pressure term giving

$$\frac{\partial v}{\partial t} = -(v\cdot\nabla)v - \frac{kT}{m} \nabla \ell n\ N + \nu\nabla^2 v + \alpha(N_i - N_b)(u - v)$$

where N_b is the background ion density, k is Boltzmann's constant, T is the neutral gas ambient temperature, m is the neutral particle mass, ν is the kinematic viscosity and α is the coupling coefficient $e/mN\mu$ discussed in Section 2.1. The above equation constitutes two relations, one relation for each component of v.

While it is probably true that the adiabatic assumption for the slightly compressible component of the neutral flow is probably closer to the actual physical situation, the isothermal assumption provides a very accurate approximation because the deflections of the density from its ambient value are very small (less than 1%). Use of the isothermal approximation leads to terms which are more straightforward to evaluate in the Navier-Stokes equation. If the adiabatic assumption were made then terms involving the evaluation of the density raised to a non-integral power would require evaluation.

Subtraction of the background density from the drag component is necessary to remove the influence of drag effects on the background. The tendency for the ambient neutral wind to decelerate in the ionosphere is probably balanced by pressure gradients and thus a removal of the background ion-neutral drag seems appropriate.

In order to assure accuracy and stability (Ames, 1977, p. 264) the time step size used for the neutral flow calculation must be fairly small. The time step must be so small that flow at the fastest expected neutral wind velocity plus the sound speed will not cross more than 70% of a grid cell. In contrast the time step used for the ion flow calculation can be significantly larger. The time step must only be small enough so that flow at the fastest ion speed will not cross more than 50% of a grid cell. Typically, in a calculation in the frame of reference of the background ions the fastest ion speed will be less than the neutral speed. The disparity between the time step required by the neutral and ion flow motivates the use of two different time

step values. In the calculational results to be presented the neutral calculation is iterated numerous (16 to 50) times for every iteration of the ion flow.

Finite difference techniques were applied using a rectangular grid of square grid cells. The problems were formulated to be symmetric around the horizontal axis and advantage was taken of this symmetry to reduce storage requirements. The sampled functions are assumed to have a planar dependence over each cell.

The boundary values of ion and neutral density and the x- and y-components of the neutral wind are all assumed to be such that the quantities have continuous normal derivatives across the boundary. The x-component of the neutral wind is further assumed to have a fixed value on the left hand boundary that is representative of the incoming neutral flow speed. The boundary value of the ion flow potential is set such that the ion motion interior to the boundary is not influenced by the boundary's presence. The potential equation is effectively solved with the free space Green's function for the problem.

The initial conditions for the neutral parameters are that the neutral density and wind components are constant. The x-component of the wind is assumed to take the value of the ion-neutral slip speed. The y-component of the wind is assumed to be initially zero. The neutral density is assumed to have an initial value of unity.

The initial value of the ion density is assumed to have a Gaussian spatial variation superimposed on a constant background of unity. The peak value of the Gaussian is three in both cases, two larger than the assumed background ion density. This value causes the ion-neutral slip to be roughly one-half of the wind

velocity which is in fair agreement with observations of these clouds. The initial e-fold radius has been set according to which release is modelled as specified in Table 3-1. Table 3-1 also lists many other important parameters used in the two simulations, the results of which are discussed in the following section.

3.2 NUMERICAL RESULTS FOR THE SIMULATIONS OF AVEFRIA DOS AND IRIS

The results of a coupled ion-neutral interactive flow calculation for a small (1.7 km e-fold) dense (3.5×10^7 el/cc peak) plasma cloud are illustrated in Figures 3-1 thru 3-13. The parameters used in the calculation are presented in Table 3-1 and were chosen to characterize the pressure and viscosity at a 200 kilometer altitude. Above each figure the contour values are given and the contours are coded such that the highest value contour is bold and the lowest value contour is dotted. The distance values in the labels are assumed to be in kilometer spatial units.

Figure 3-1 shows contours of the initial plasma density. The initial density profile has a Gaussian spatial dependence which is centered to the left hand side of the grid. The neutral wind is initially directed toward the right and centering the cloud to the left allows for advancement of the simulation to later times without moving the frame of reference. The neutral flow is calculated for the first sixteen neutral time steps

Table 3-1

Simulation Parameters

	Avefria Dos	IRIS	Units
Initial Values			
Radius--R_o	1.7	5	km
Neutral wind--v_x	125	55	m/sec
Neutral Parameters and Coefficients			
Pressure--kT/m	3.4×10^5	2.4×10^5	m^2/sec^2
Viscosity--ν	1.6×10^5	5.3×10^4	m^2/sec
Coupling--α	1×10^{-11}	6×10^{-12}	m^3/sec
Peak density (implied by α)	3.5×10^7	2×10^7	particles/cc
Reynolds number ($R_o v/\nu$)	1.3	5.2	
Sampling Parameters			
Grid	42×24	32×28	x by y
Total Distance	20×11.4	47×41.1	km in x by km in y
$\Delta x = \Delta y$	476	1,469	meters
Δt_{ion}	2	10	seconds
$\Delta t_{ion}/\Delta t_{neutral}$	16	50	

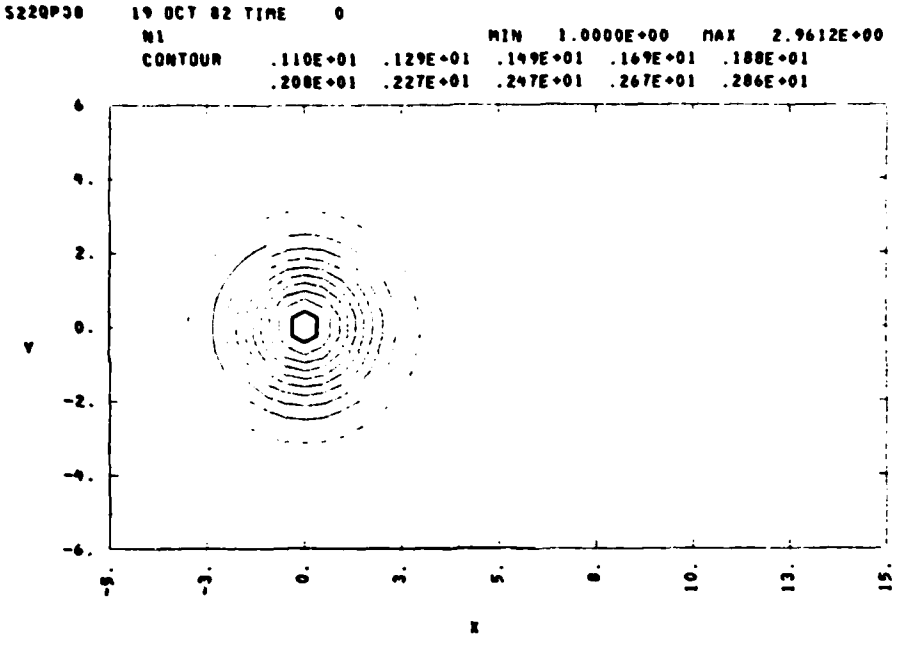

Figure 3-1. Initial plasma density for Avefria Dos calculation.

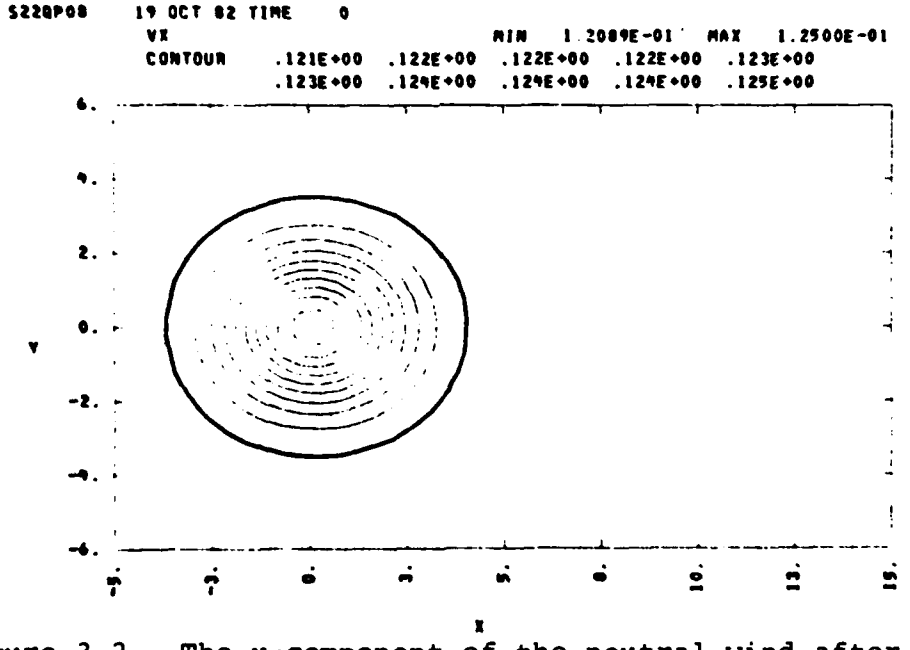

Figure 3-2. The x-component of the neutral wind after 10 seconds of initial evolution. Units are km/second.

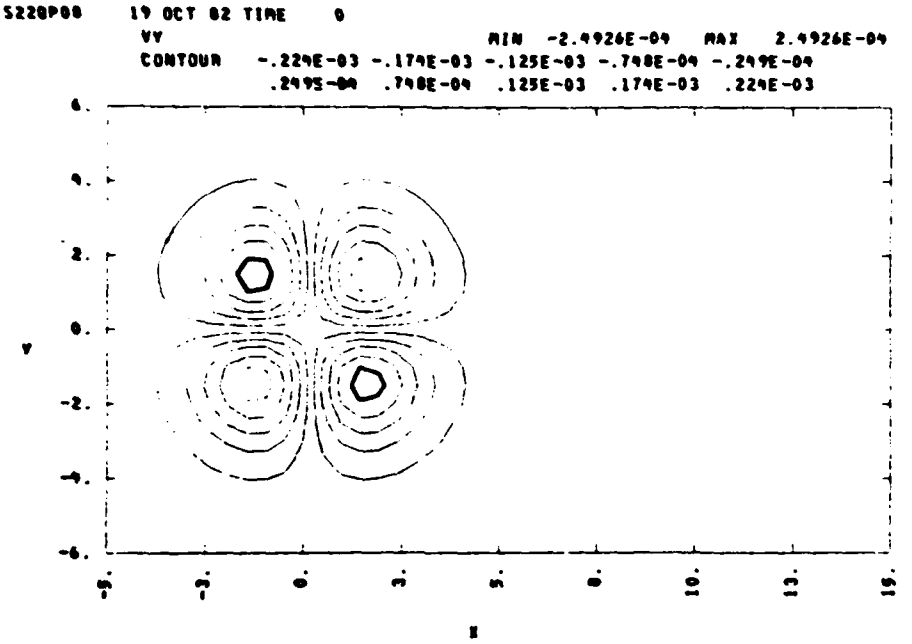

Figure 3-3. The y-component of the neutral wind after 10 seconds of initial evolution.

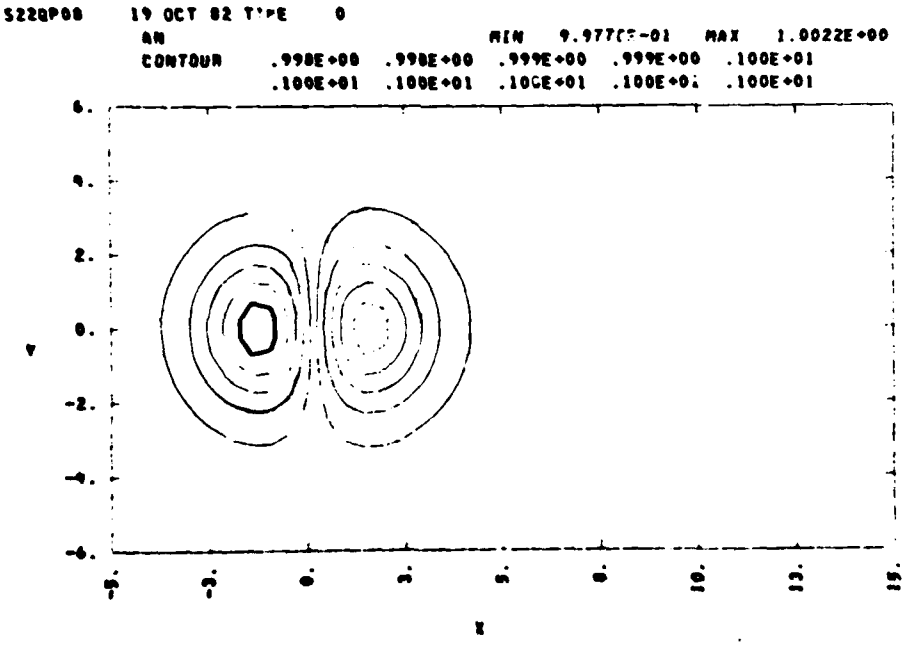

Figure 3-4. The neutral density after 10 seconds of initial evolution.

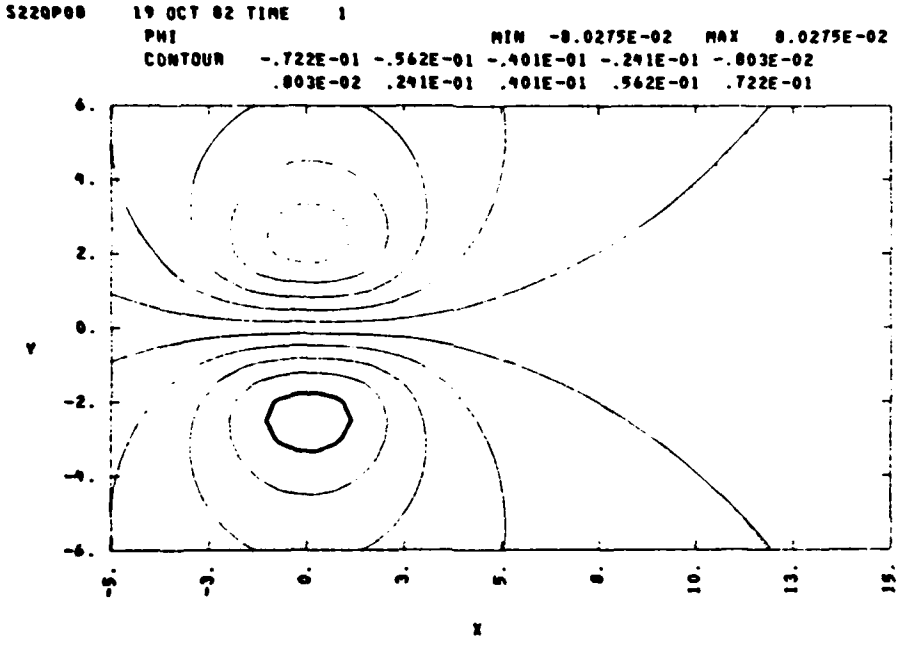

Figure 3-5. The electrostatic potential resulting from initial plasma density and initial wind values.

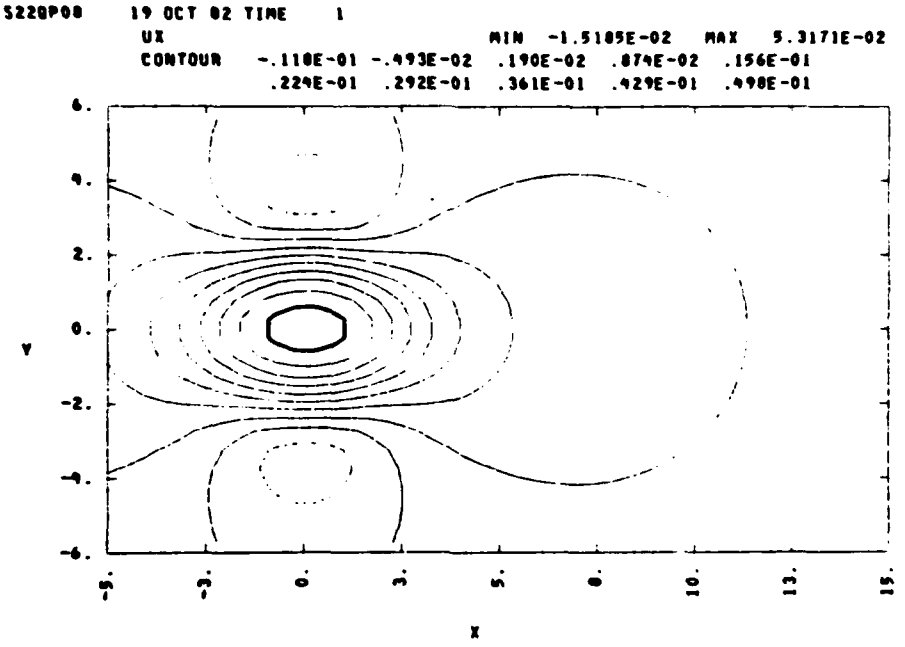

Figure 3-6. The x-component of the initial ion velocity. Units are km/sec.

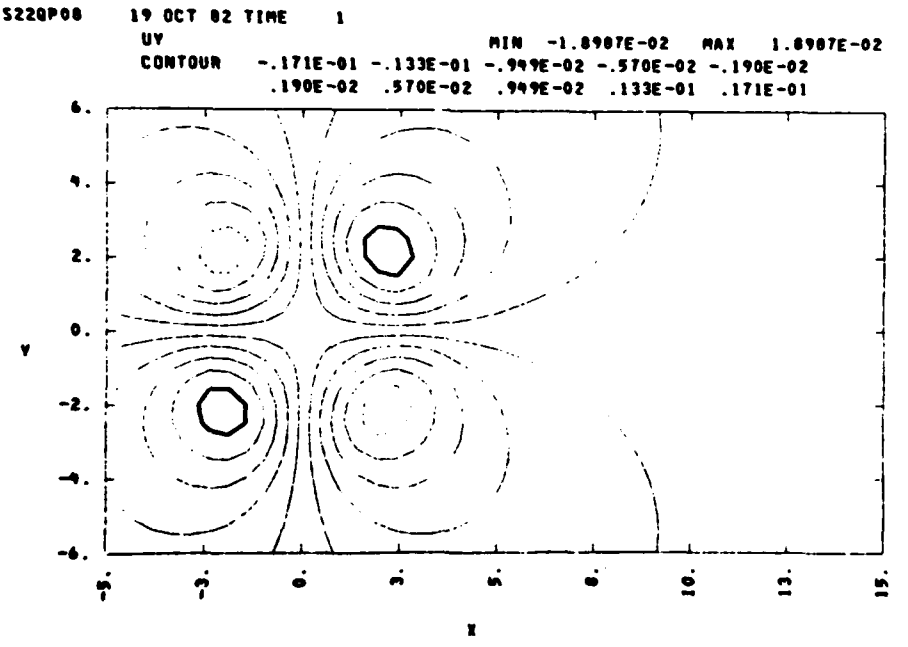

Figure 3-7. The y-component of the initial ion velocity.

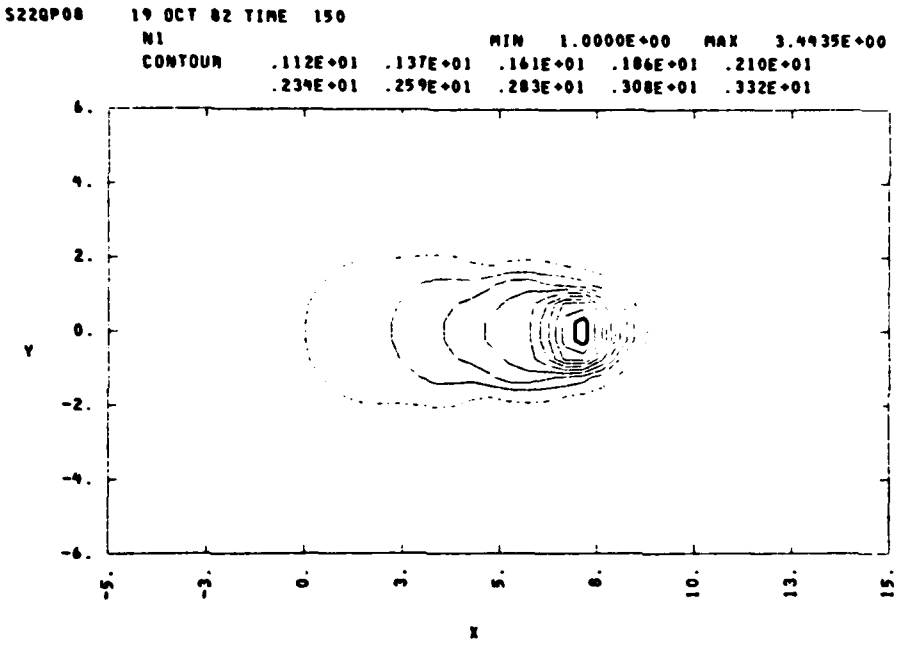

Figure 3-8. The plasma density after 150 seconds of evolution.

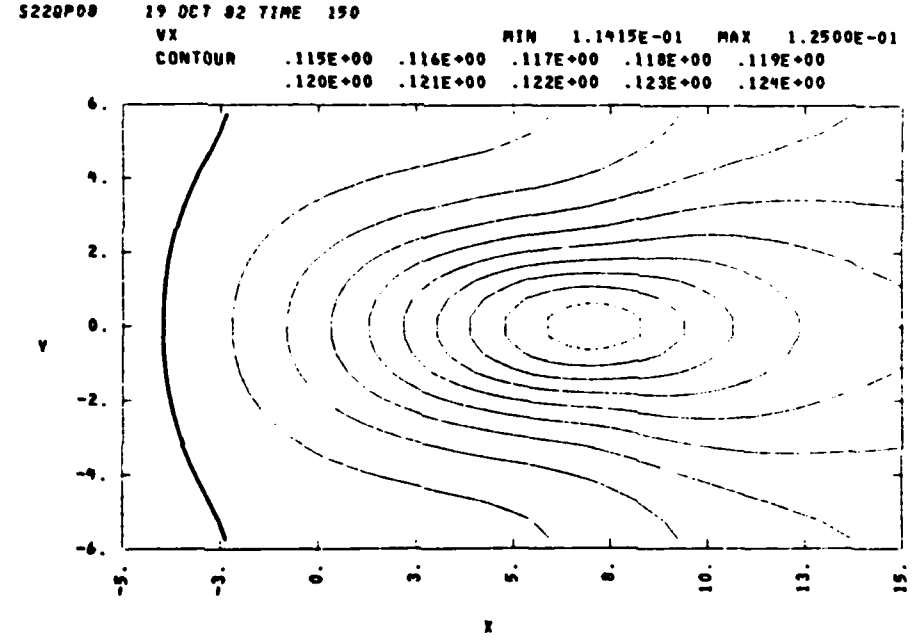

Figure 3-9. The x-component of the neutral wind after 150 seconds of evolution. The wind drag effect creates a 10 meter/second decrease.

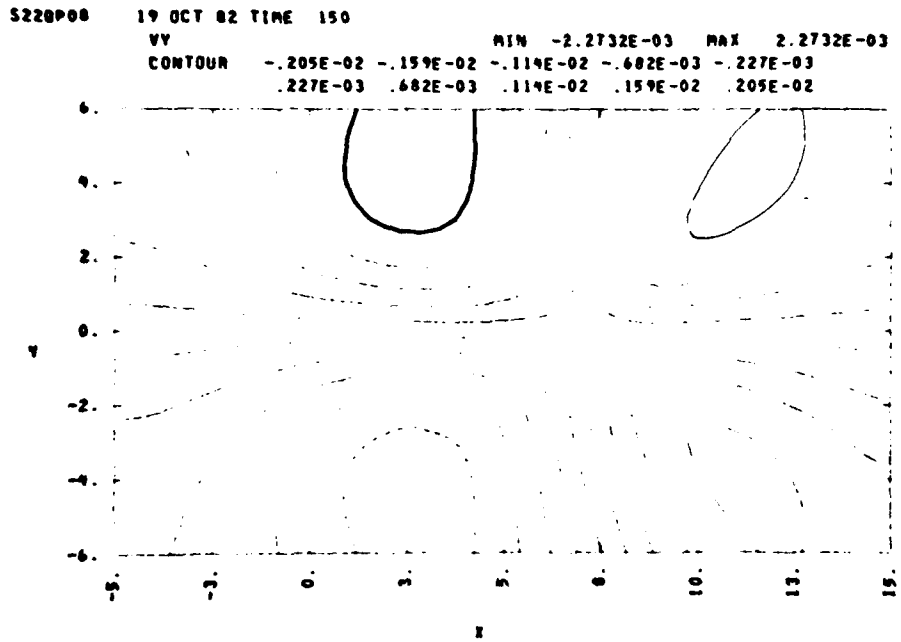

Figure 3-10. The y-component of the neutral wind after 150 seconds of evolution.

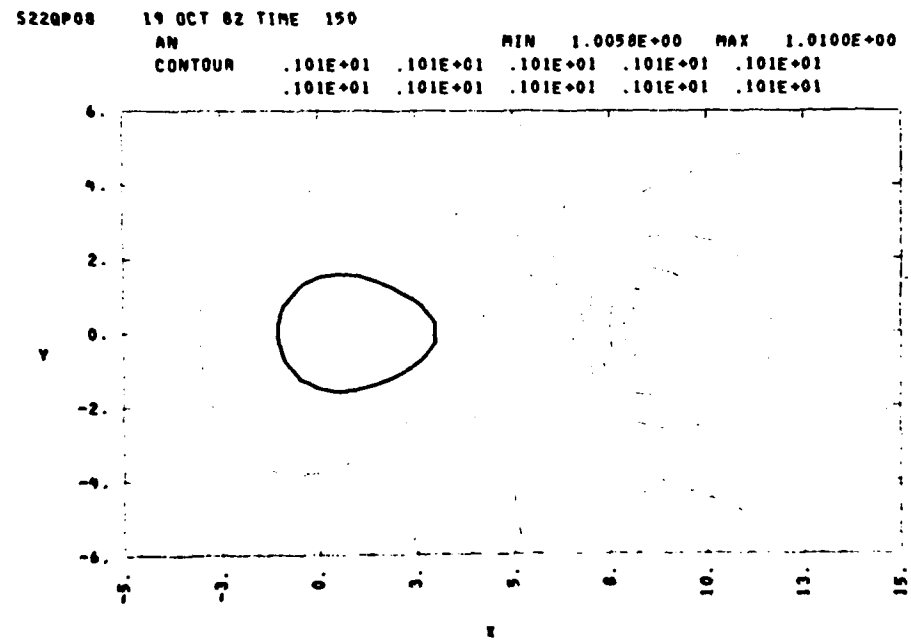

Figure 3-11. The neutral density after 150 seconds of evolution.

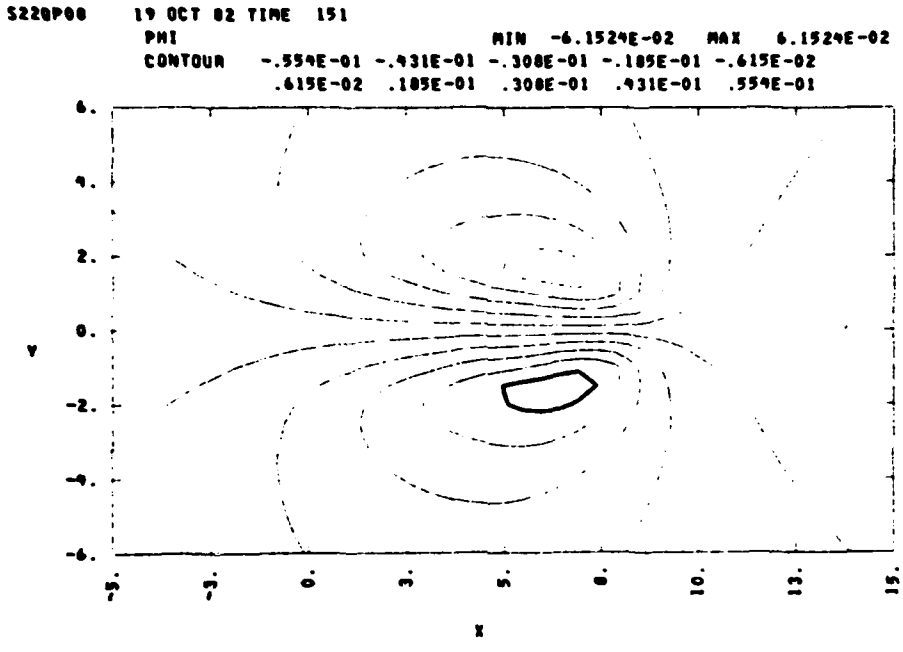

Figure 3-12. The electrostatic potential after 150 seconds of evolution.

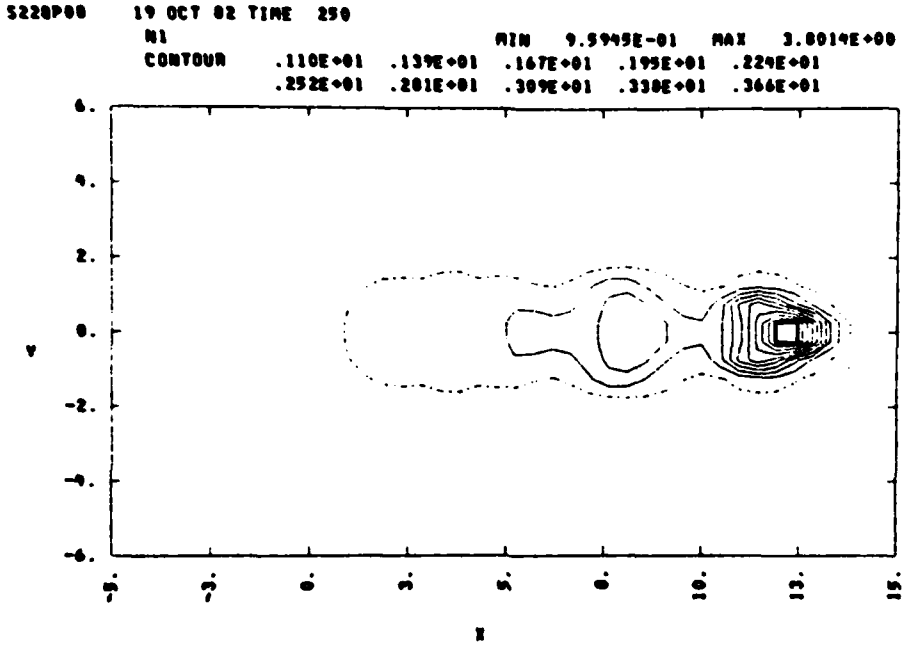

Figure 3-13. The ion density after 150 seconds of evolution.

assuming the plasma velocity is zero. Plots of the resultant neutral flow parameters are shown in Figures 3-2 thru 3-4. The neutral wind values are then used to determine the electrostatic potential shown in Figure 3-5. Because the free space boundary condition algorithm has been used the resultant potential is not affected by the fairly close grid boundary. The plasma velocity components implied by the potential are shown in Figures 3-6 and 3-7. The maximum value of the x-component of the plasma velocity is 53 meters per second, roughly one-half of the initial 125 meter per second neutral wind speed. The ion neutral slip speed is, thus, roughly 70 meters per second through the maximum ion density with higher slip speeds occurring elsewhere. For subsequent neutral flow iterations the ion flow velocities are used to determine the drag force, instead of assuming stationary ions as is done in the initial time step.

Figures 3-8 thru 3-12 depict the calculated ion and neutral parameters after 150 seconds of evolution. The evolution depicted shows little influence of the ion neutral coupling effect because the change in the neutral wind is fairly small. The calculation indicates a change of only 11 meters per second. This small value disagrees with a 60 meter per second value predicted using the drag effect relations of Section 2.1, however, those relations neglect viscous forces. A comparison of viscous forces to drag forces reveals that for this problem viscosity is the velocity determining force, as might be expected because of the low Reynolds number. Because of the viscous forces Avefria Dos should evolve in a manner that is insensitive to ion-neutral drag

effects and the results of past electrostatic analyses including McDonald et al. (1979) should apply.

It may be worthwhile to point out a discrepancy between the calculated results and the observations and data presented in McDonald et al. (1979). In the calculated results shown in Figure 3-8 an elongation of the cloud can be noted that is of order 2 1/2 to 1. Cloud elongation is a function of the slip velocity which is itself a function of the peak-to-background ratio and the wind speed. The parameters were chosen according to McDonald et al.'s (1979) range of acceptable values and yet the cloud elongation is much more severe than that observable (≈1 1/2 to 1) in the optical data also published in McDonald et al. (1979). The implication of the discrepancy is that the peak-to-background ratios found acceptable by McDonald et al. (1979) based on cloud structuring properties may not be reflective of the observed cloud dynamics which were not monitored in McDonald et al. (1979). Indeed, peak-to-background ratios of 2 or less (in place of the value of 3 currently modelled) would be appropriate to model cloud dynamics. These low values lie outside the acceptable range presented in McDonald et al. (1979), suggesting that the structuring of Avefria Dos may not be fully explained.

Figure 3-13 shows the plasma density after 250 seconds of evolution. By this time numerical difficulties are becoming apparent however there is still no evidence of the dimpling effects expected from ion-neutral coupling.

The results of a coupled ion-neutral interactive flow calculation for a large (5 kilometer e-fold) plasma cloud at a lower altitude (170 kilometers) are shown in

Figures 3-14 thru 3-34. The calculation assumes that the peak ion density is 2×10^7 el/cc. Note that at early time this value is probably appropriate for a barium cloud similar to the IRIS event of PLACES (Linson and Baxter, 1977) (which was similar in many respects to ESTHER of STRESS and SPRUCE of SECEDE-II), however, at later time this peak value is decreased through diffusion along the geomagnetic field line--an effect not modelled in this calculation.

The initial values of ion density are shown in Figures 3-14. The values of the neutral wind x- and y-components and the neutral density perturbation produced by 10 seconds of flow through this stationary plasma distribution are shown in Figures 3-15 thru 3-17. Note that the x-component of the neutral wind drops by 5 meters per second during this initial interval. The electrostatic potential and the x- and y-components of the plasma velocity are shown in Figures 3-18 thru 3-20. The qualitative nature of these contour plots is very similar to the initial values obtained for the Avefria Dos calculation indicating that the effects of ion-neutral wind drag make little difference to the initial cloud evolution. Note that the initial x-component of the plasma velocity is 21 meters per second indicating a slip speed of roughly 35 meters per second at the peak density value. This slip speed is in agreement with the slip speed observed during IRIS.

Figure 3-21 shows the plasma density after 150 seconds of evolution. At this time only a small amount of contour distortion has occurred. Because of the

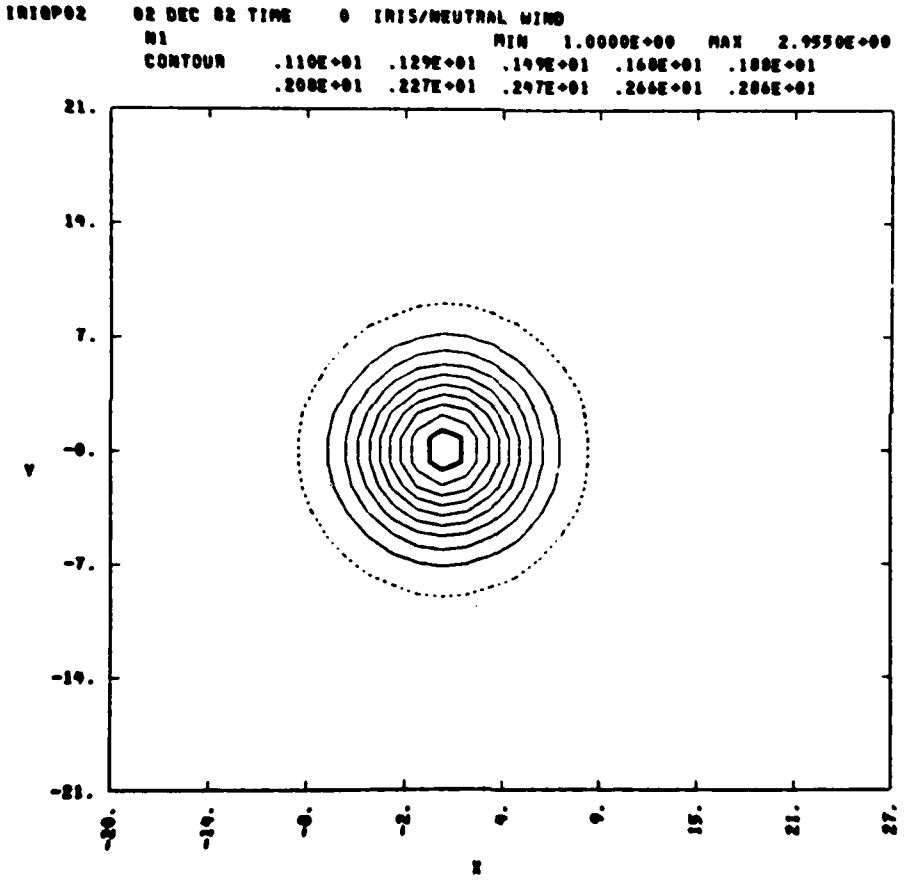

Figure 3-14. Initial ion density for coupled ion-neutral flow calculation of IRIS.

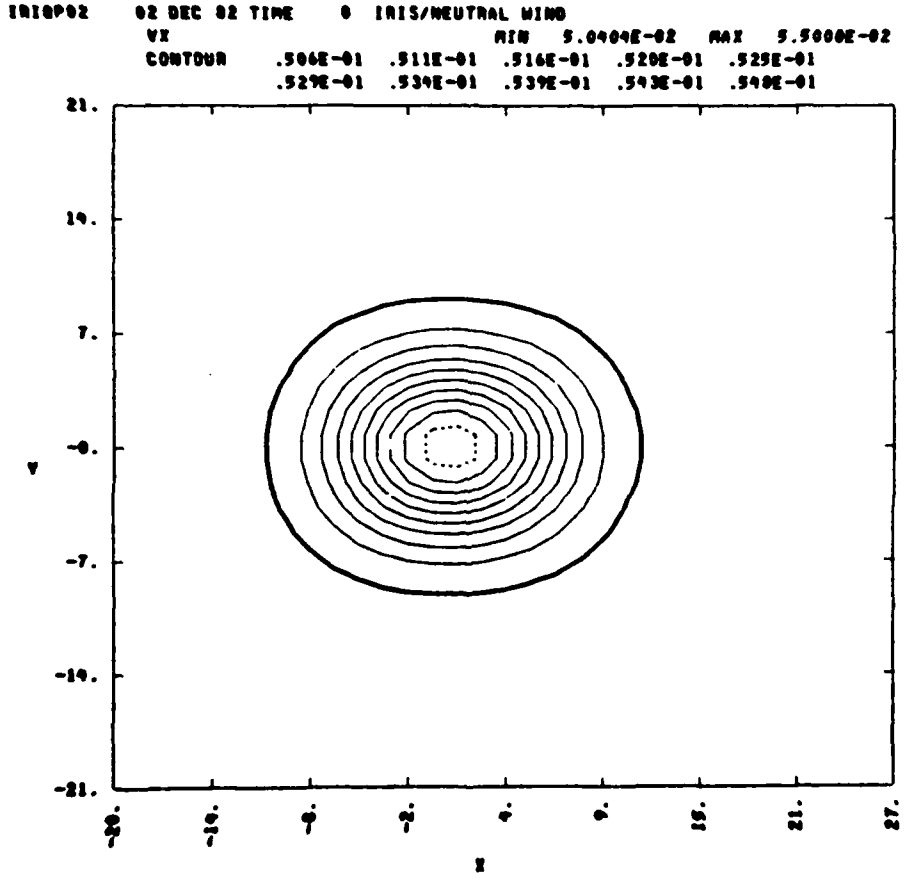

Figure 3-15. The x-component of the neutral wind after the first time step.

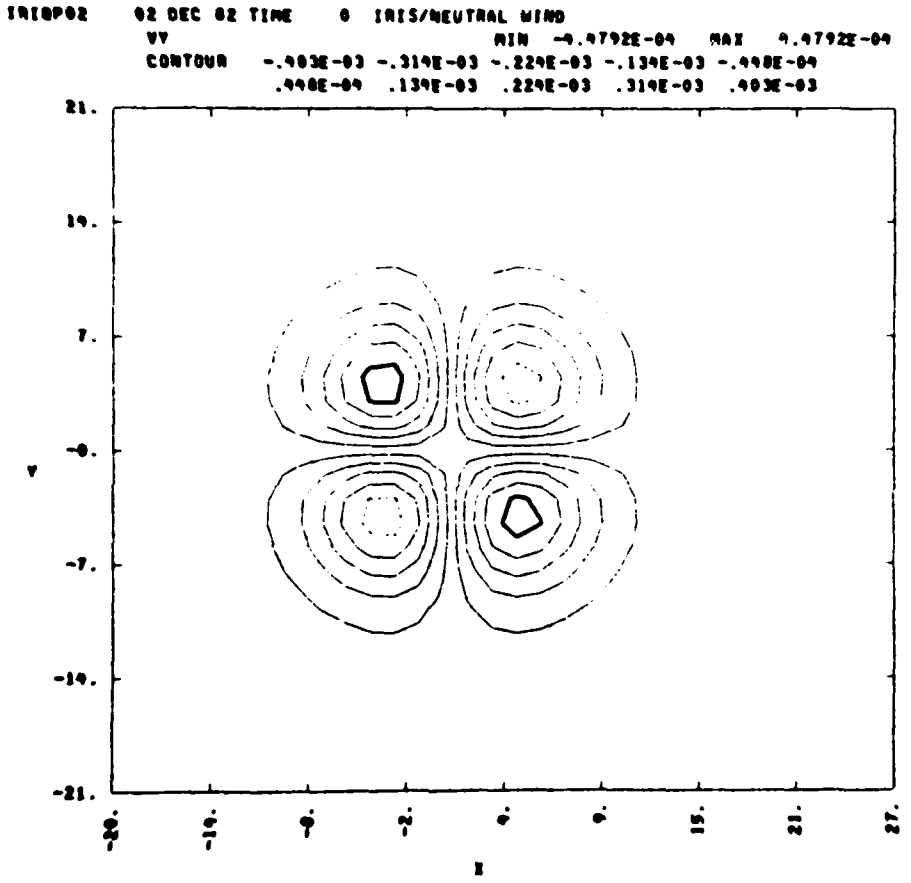

Figure 3-16. The y-component of the neutral wind after first time step.

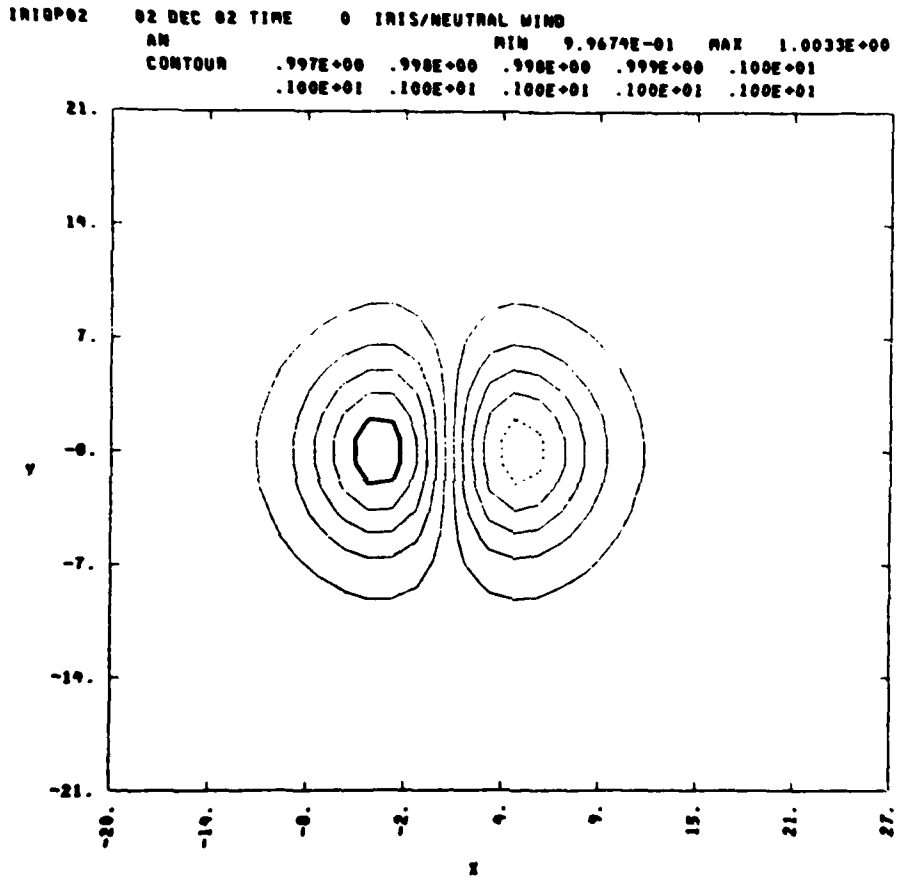

Figure 3-17. The neutral density after the first time step.

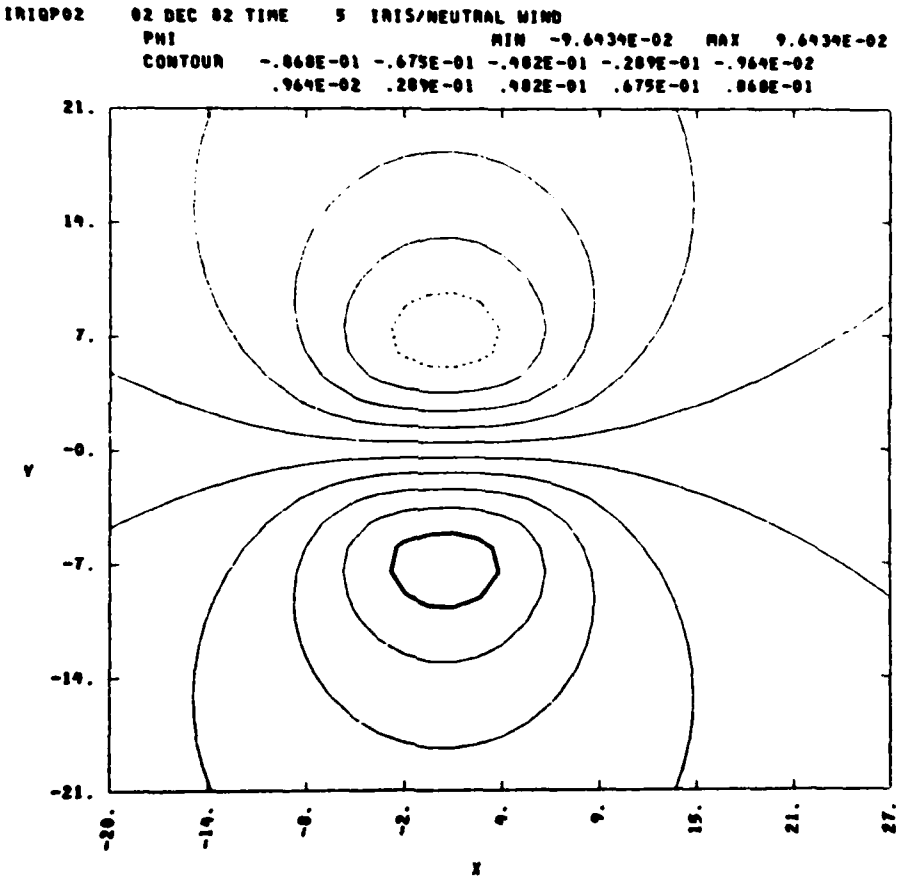

Figure 3-18. The results of the first time step electrostatic potential calculation.

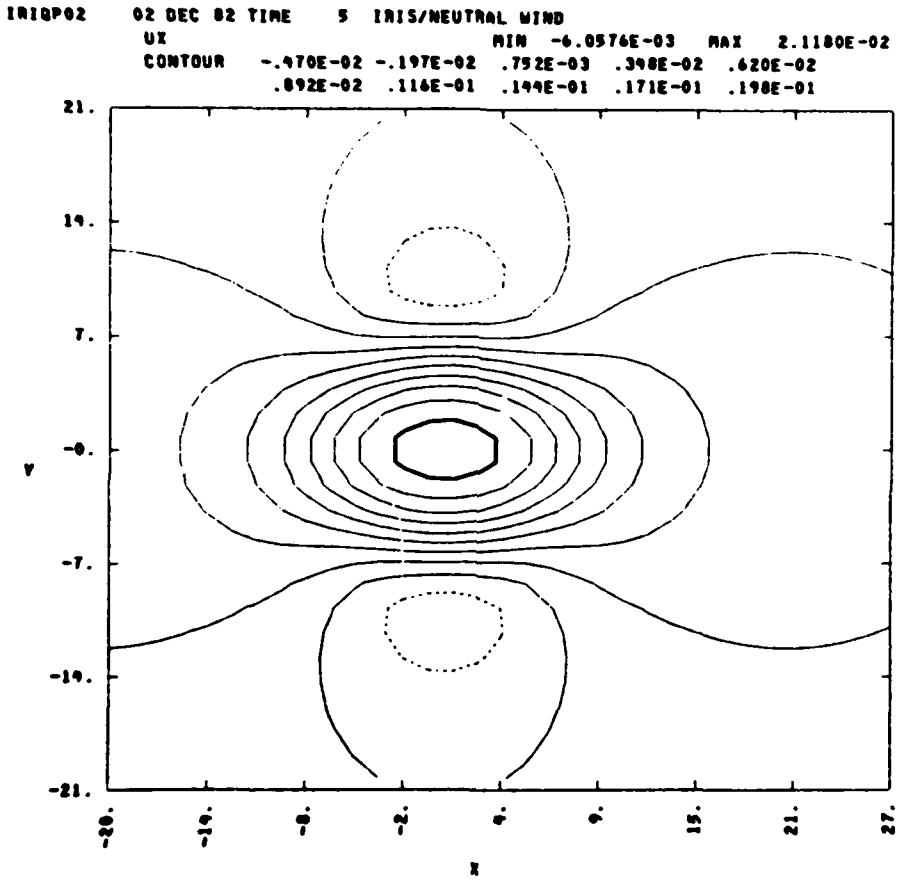

Figure 3-19. The initial x-component of the plasma velocity.

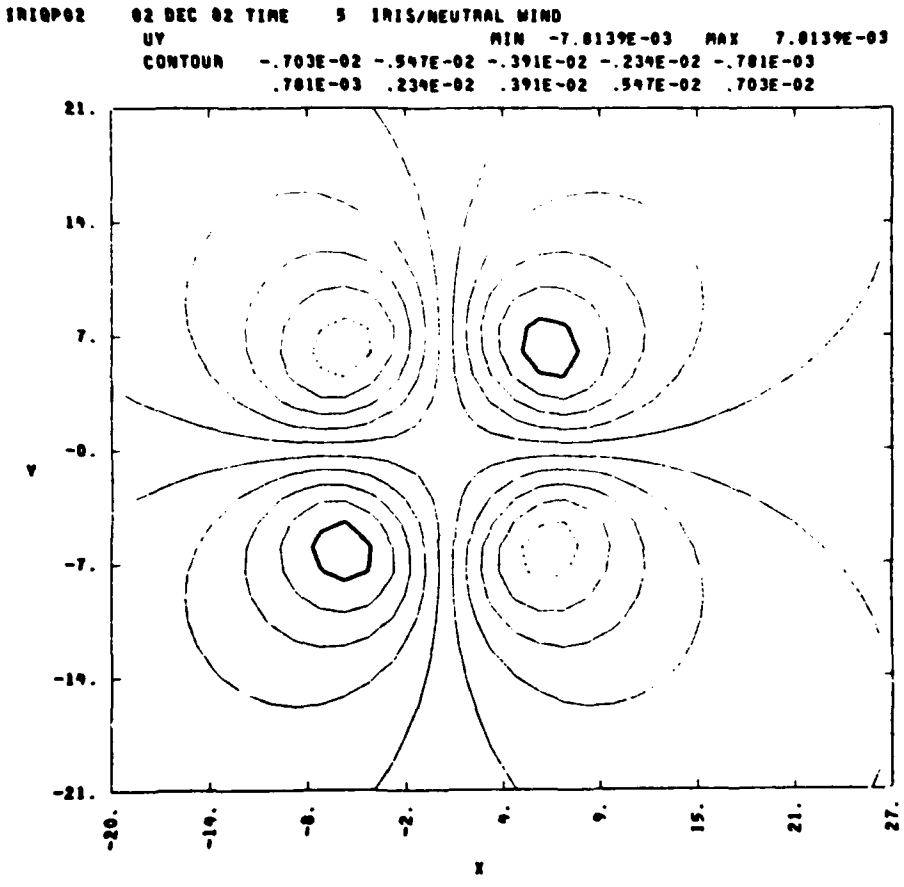

Figure 3-20. The initial y-component of the plasma velocity.

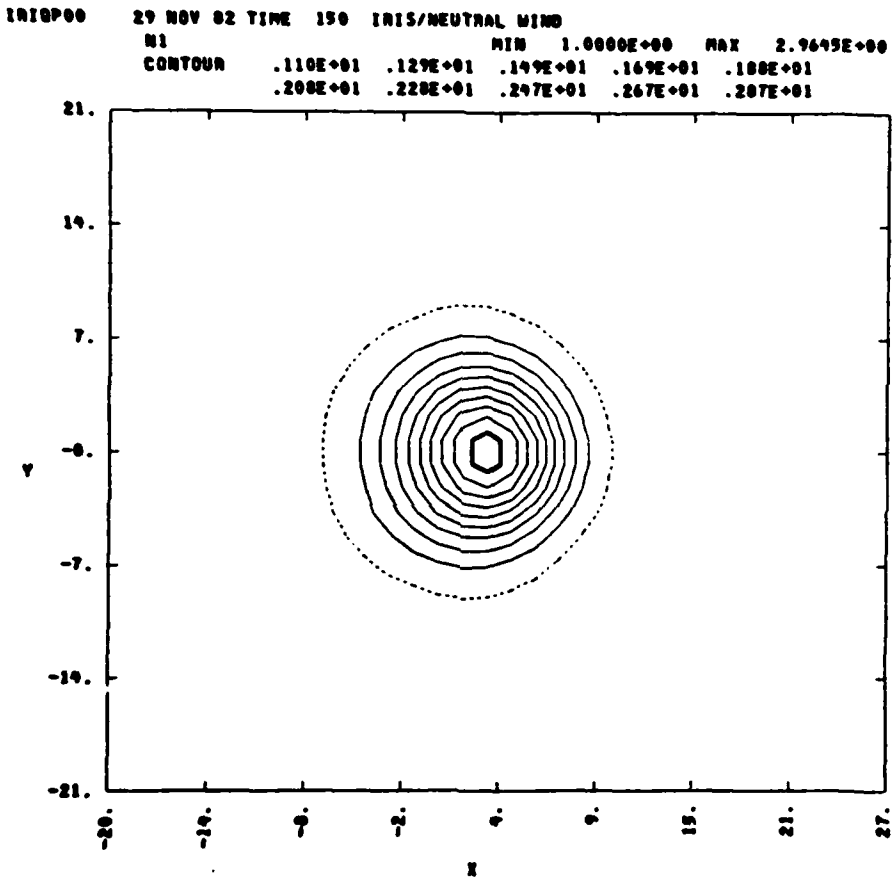

Figure 3-21. The plasma density after 150 seconds of plasma evolution.

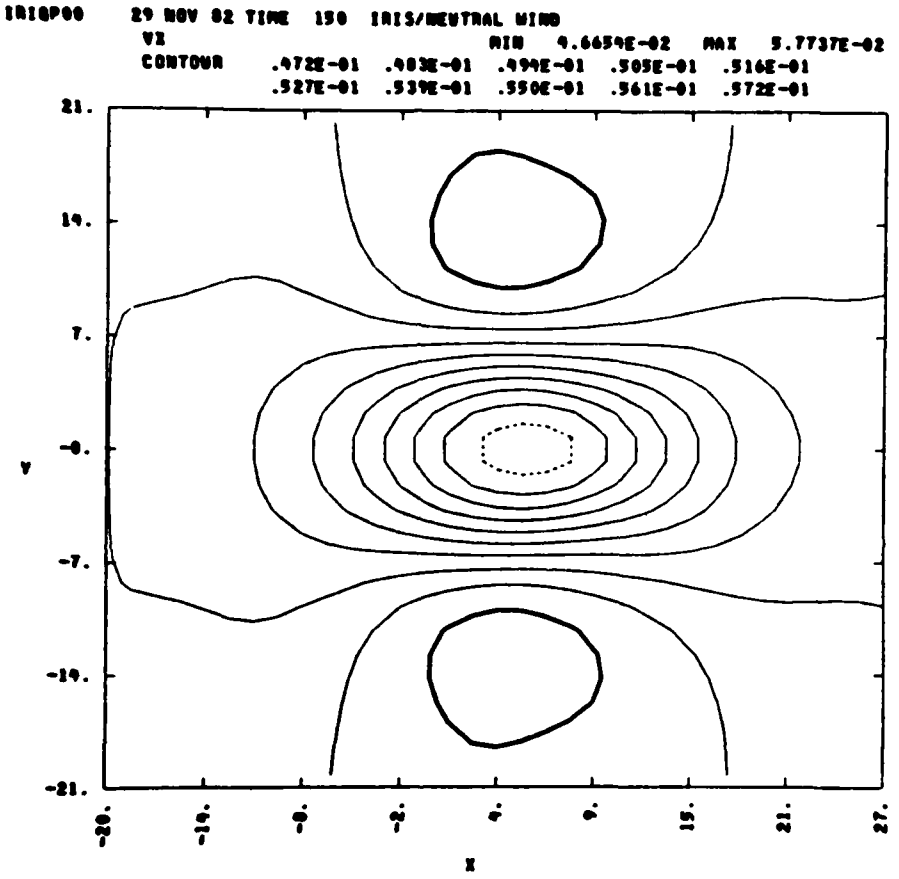

Figure 3-22. The x-component of the wind after 150 seconds of plasma evolution.

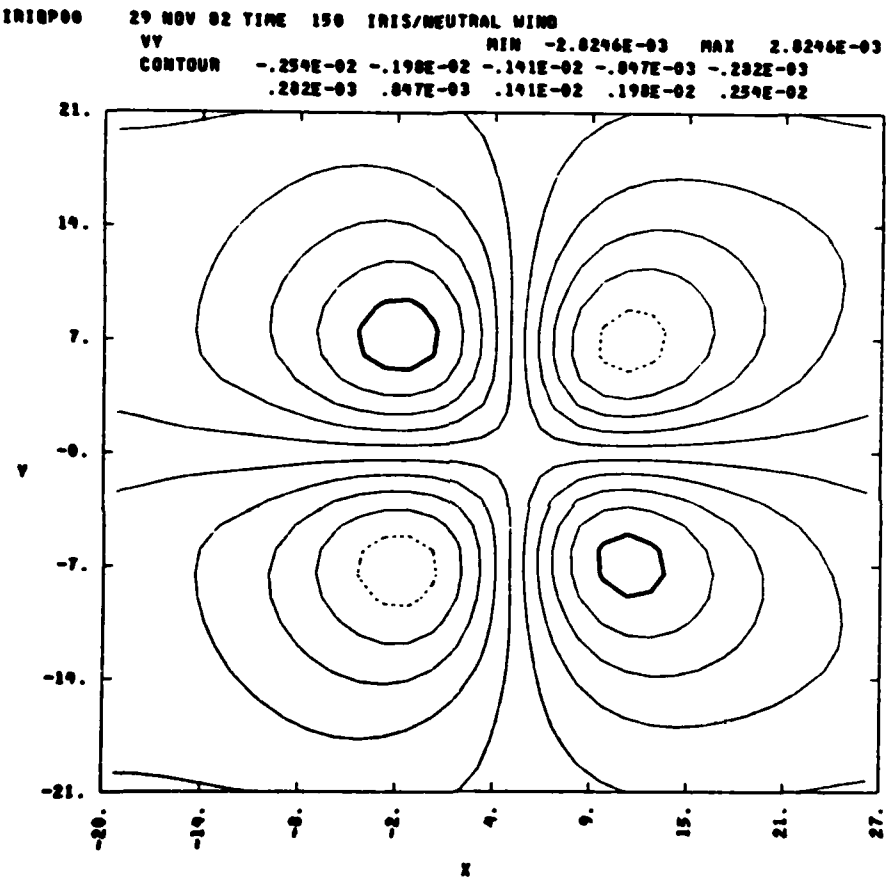

Figure 3-23. The y-component of neutral velocity after 150 seconds of evolution.

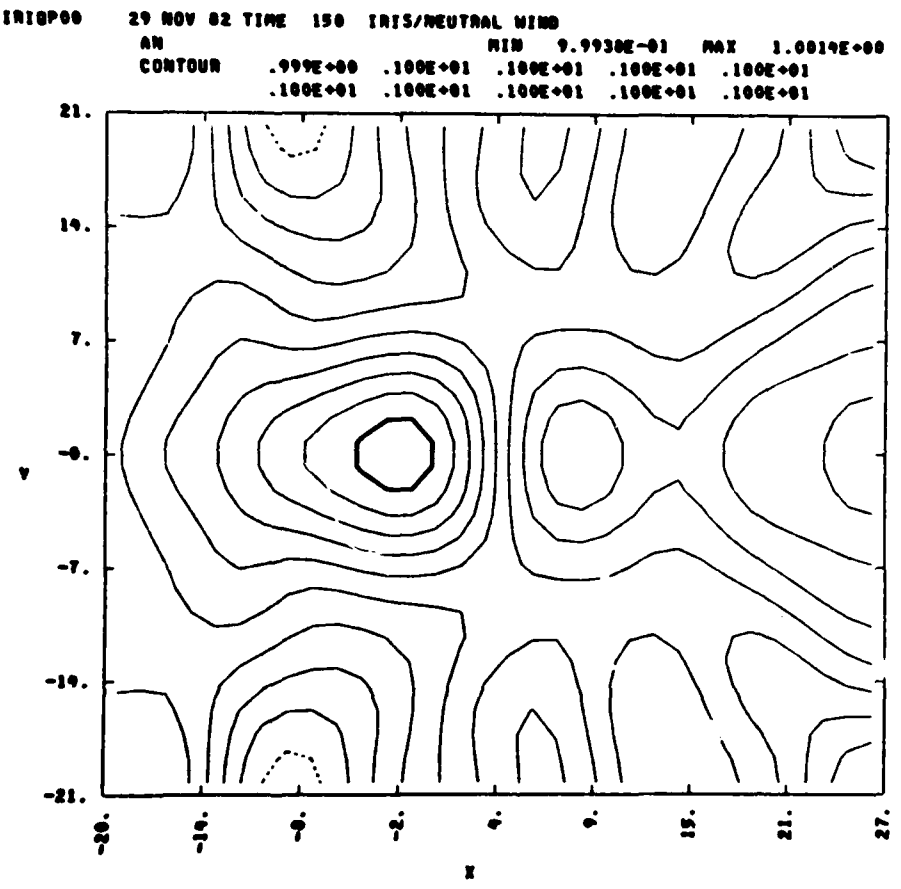

Figure 3-24. The neutral density after 150 seconds of evolution.

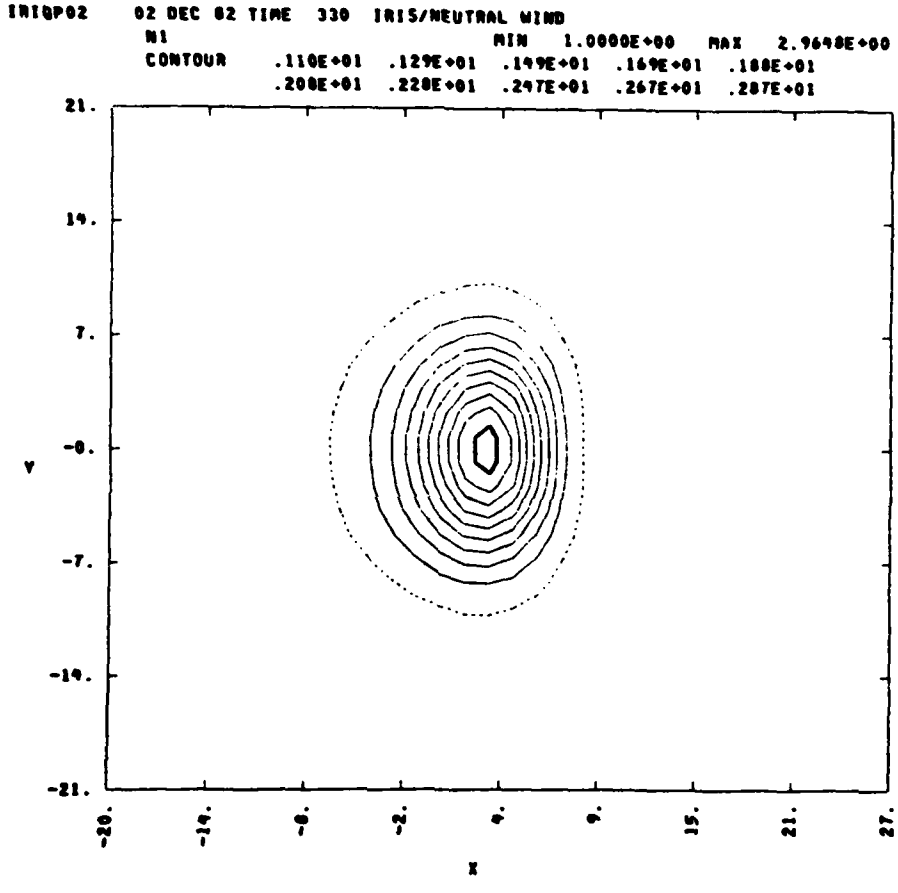

Figure 3-25. The plasma density after 330 seconds of evolution.

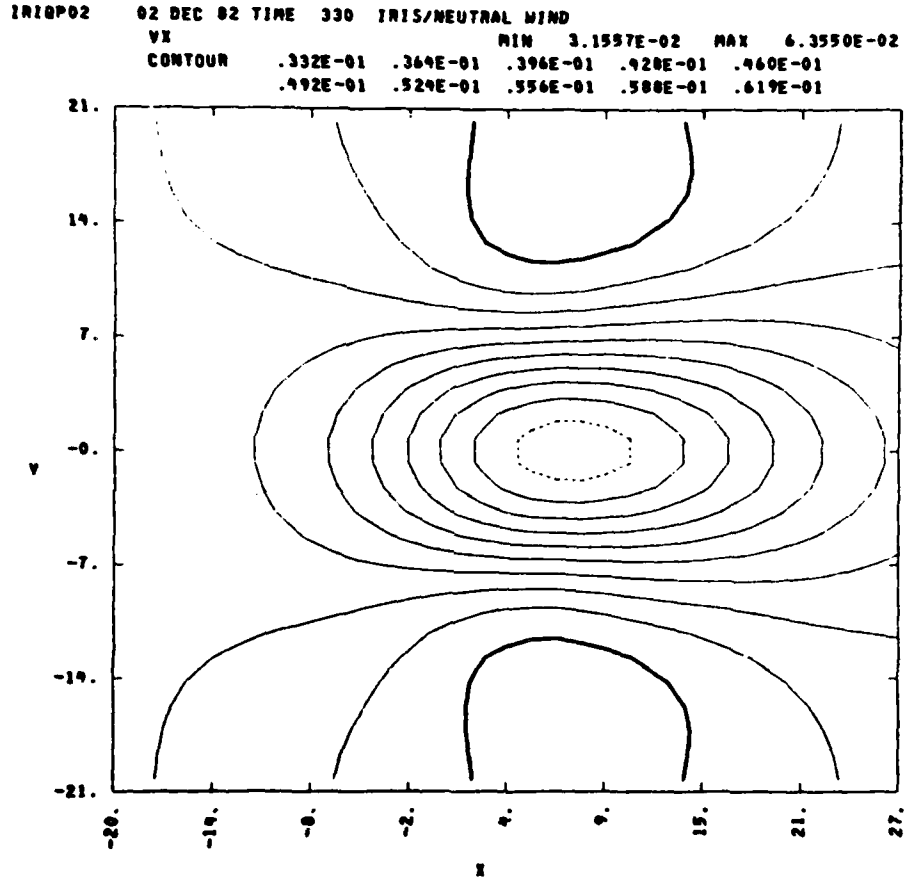

Figure 3-26. The x-component of the neutral wind after 330 seconds of evolution.

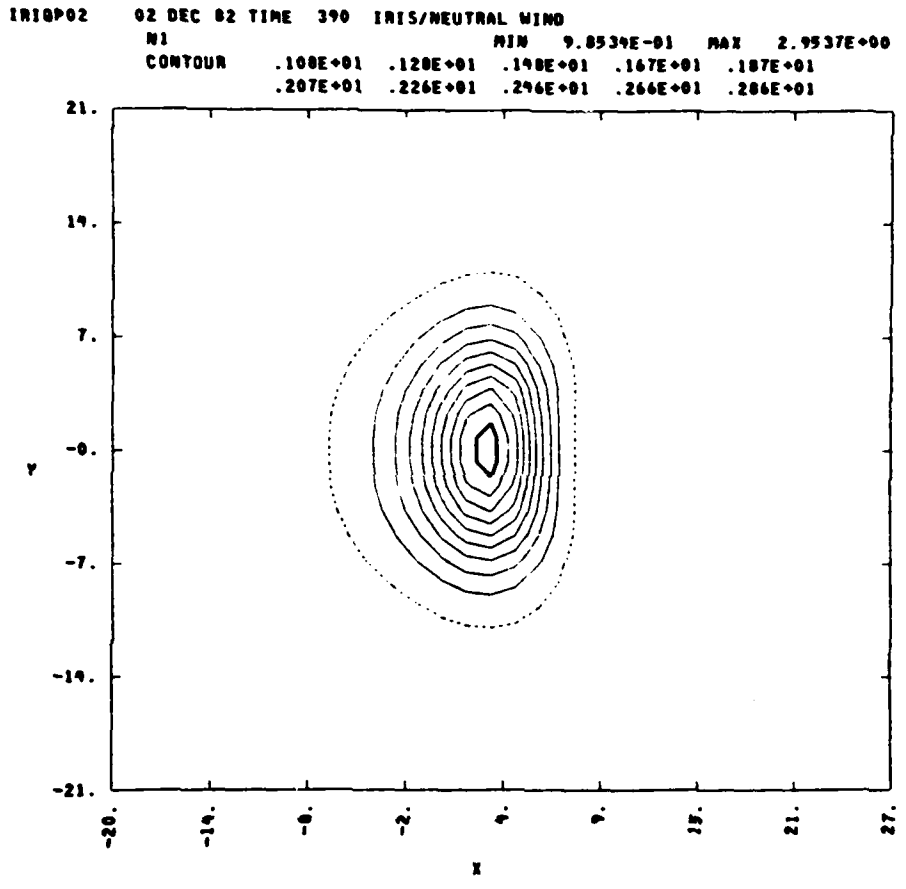

Figure 3-27. The ion density after 390 seconds of evolution. Dimpling of the lowest density contour is evident.

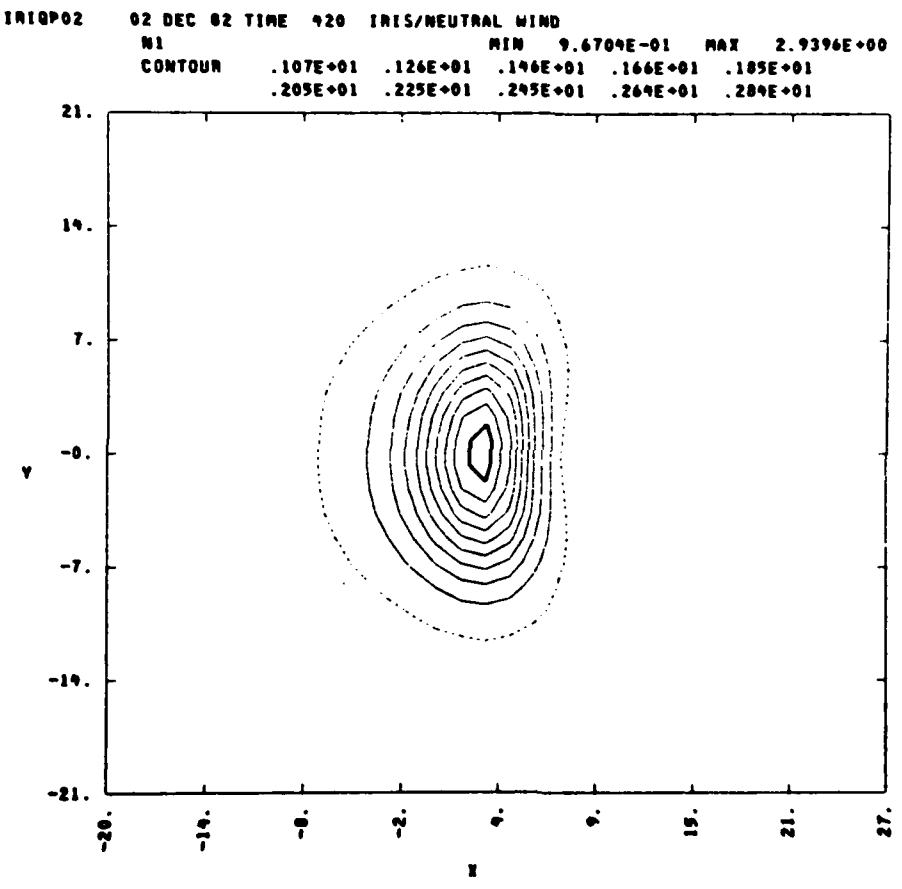

Figure 3-28. The plasma density after 420 seconds of evolution.

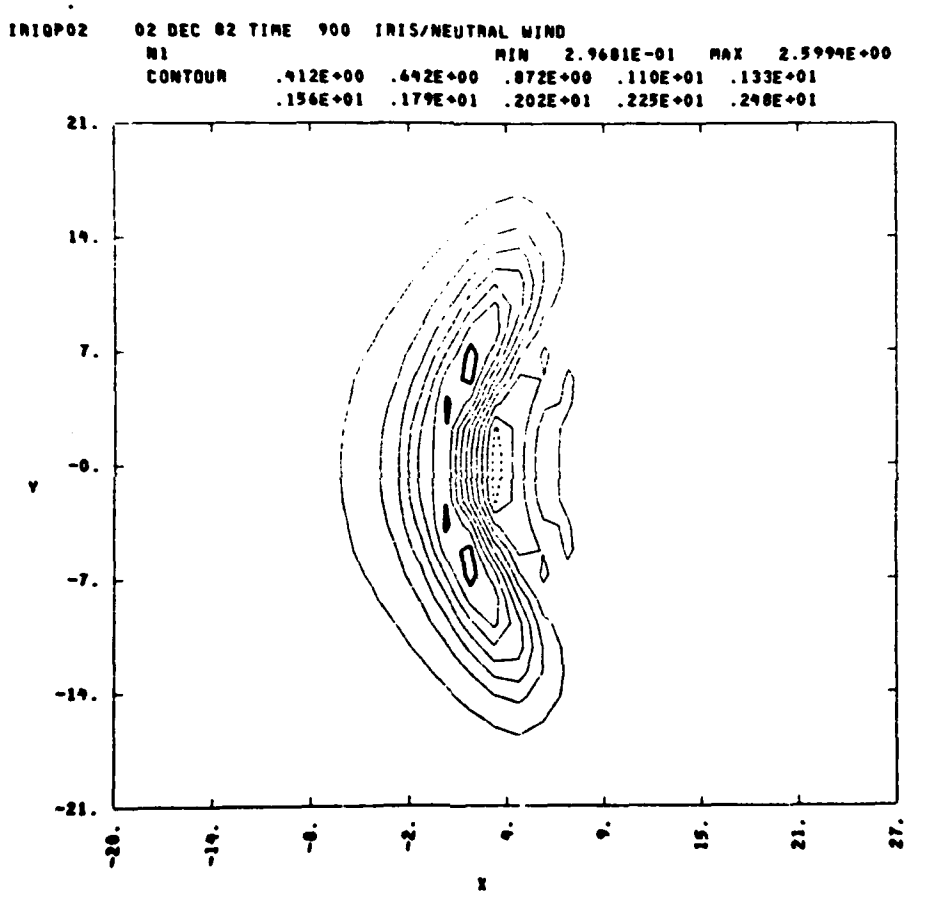

Figure 3-29. The ion density after 900 seconds of evolution. Isolated peak values and density depletions are indicative of numerical difficulties at this late time.

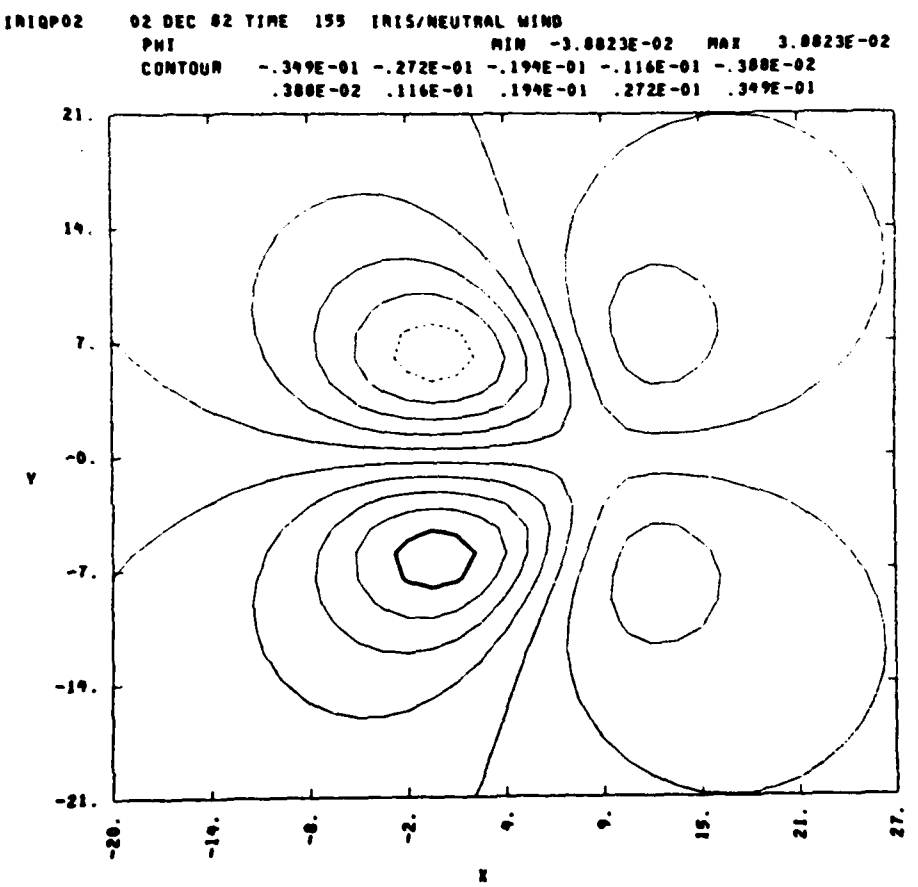

Figure 3-30. Electrostatic potential at 155 seconds. Quadripole nature is evident.

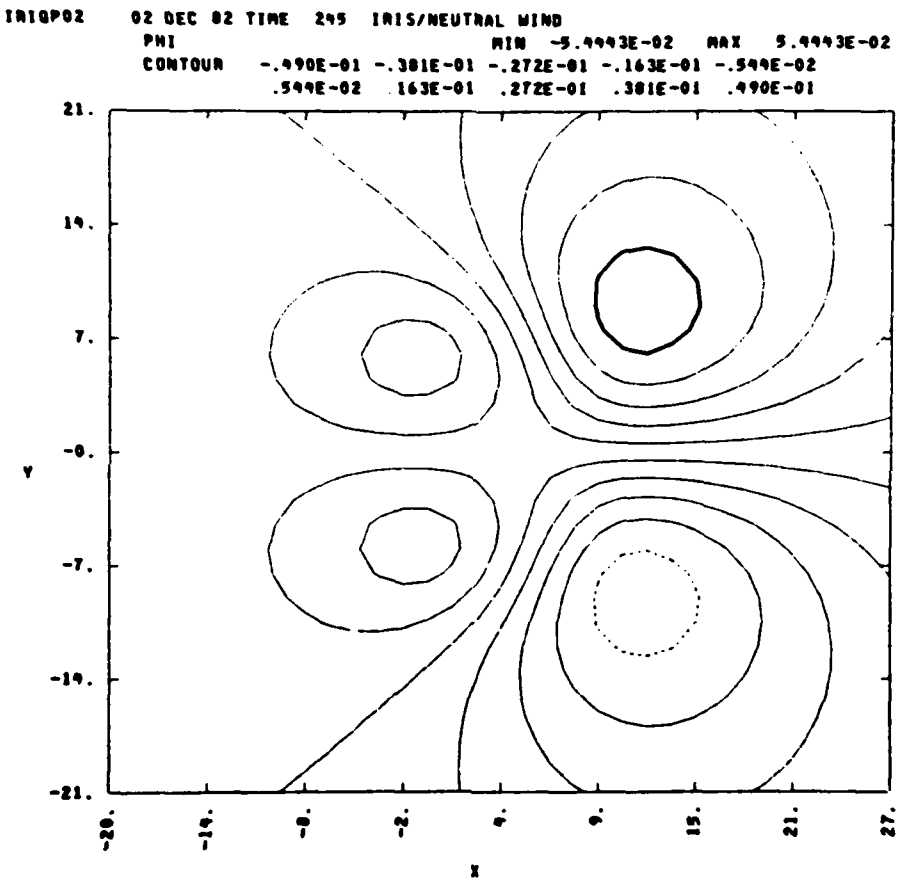

Figure 3-31. Electrostatic potential at 245 seconds.

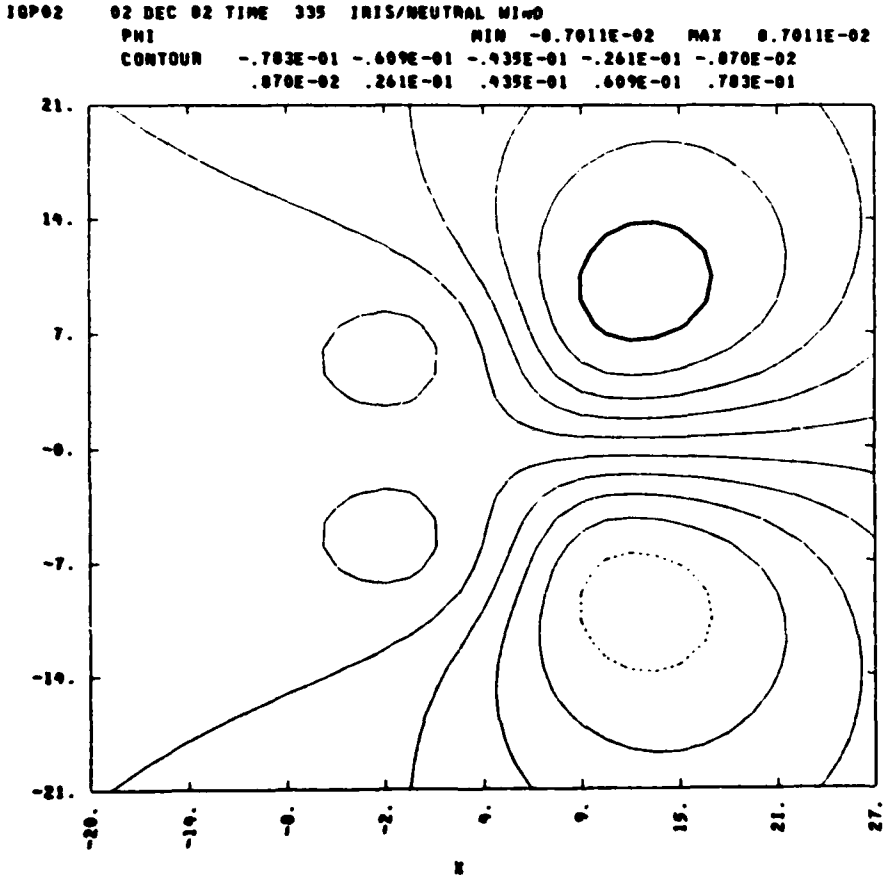

Figure 3-32. Electrostatic potential at 335 seconds.

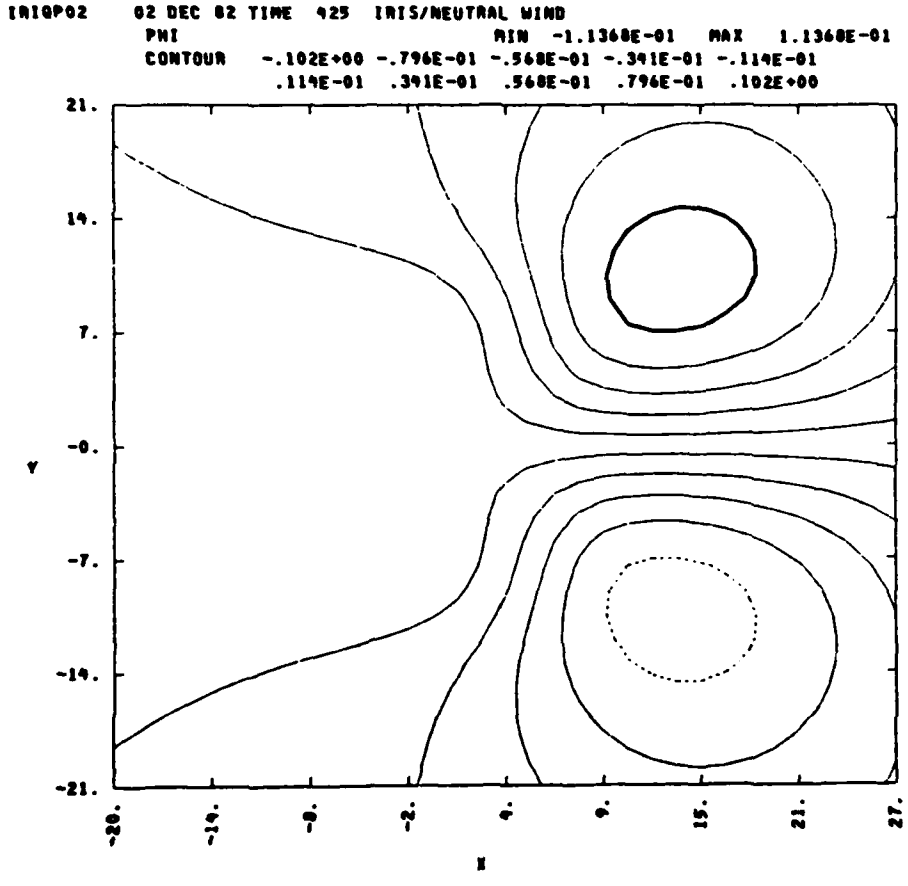

Figure 3-33. Electrostatic potential at 425 seconds. The dipole associated with the wake has completely dominated the dipole polarization associated with the cloud.

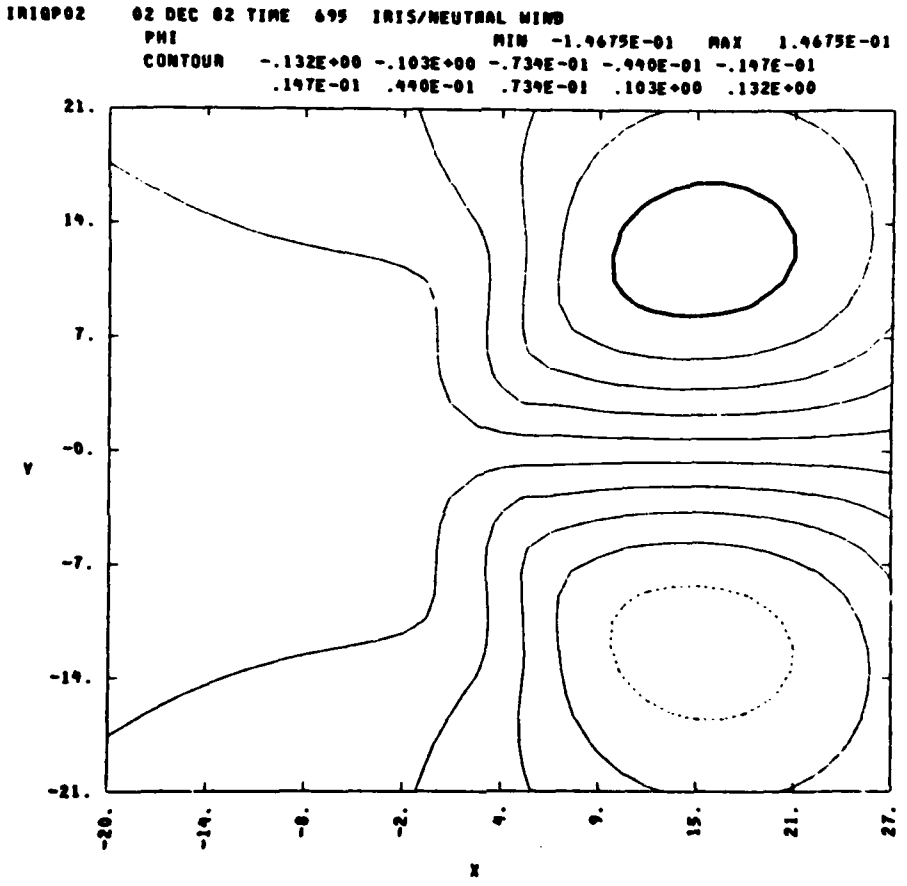

Figure 3-34. Electrostatic potential at 695 seconds.

lesser wind velocity this cloud evolves slower than Avefria Dos.

The neutral flow parameters at 150 seconds are shown in Figures 3-23 thru 3-24. These quantities are also still evolving. The decrease in the x-component of the neutral wind is only 9 meters per second at this time.

The plasma density and x-component of the neutral wind at 330 seconds are shown in Figures 3-25 and 3-26. This time is roughly equivalent to the 150 second time in the Avefria Dos evolution based upon proportional scaling to the neutral wind. The distortion of the ion cloud is now significantly different from that of Avefria Dos because of the ion-neutral coupling effect.

At the 330 second time the neutral wind has nearly reached a steady flow situation. The decrease in the neutral wind is 23 meters per second. This value reflects a balance between ion drag and neutral wind momentum loss and to a lesser extent the viscosity.

In Section 2.1 the decrease in the neutral wind considering only the momentum term is given. Simple approximations to the flow pattern can be made to derive another useful relation which also accounts for viscosity and ion-neutral slip. The resulting relation is

$$\Delta v = \frac{\alpha N_d}{\alpha N_d + 2\nu/R_o^2 + v/2R_o} v_{slip}$$

where α is the coupling coefficient, N_d is the peak ion density minus the background density, R_o is the e-fold radius, v is the ambient wind speed in the

frame of the background ions, and v_{slip} is the ion-neutral slip value at the peak density position. The factor of 2 which is present in the viscosity term of the denominator arises from the second derivative of an assumed Gaussian spatial variation in the y-direction for the x-component of the neutral wind. The factor of 2 which appears in the momentum term of the denominator accounts for the fact that the change in speed occurs roughly across the complete diameter of the cloud. For the results of Figure 3-26 the Δv predicted is 19 meters per second using the parameters $\alpha = .006$, $N_d = 2$, $\nu = .053$, $R_o = 5$, $v = .055$ and $v_{slip} = 35$ meters per second. This prediction is in reasonable agreement with the Δv of 23 meters per second observed.

Continued evolution of the ion cloud is shown in Figures 3-27 thru 3-29. Evidence of the dimpling process becomes apparent at 390 seconds as shown in Figure 3-27. This dimpling becomes more pronounced at 420 seconds in Figure 3-28 and remains until later time. Figure 3-29 shows the predicted ion cloud at the final time step calculated, namely, 900 seconds. Note that numerical difficulties have arisen as evidenced by the presence of plasma depletions and by the numerous isolated regions of peak density; however, no significant change in the nature of the evolution has arisen. Also note that it is not realistic to expect the high levels of ion-neutral coupling being modelled to actually be present in IRIS, ESTHER, or SPRUCE to these late times because diffusion along the geomagnetic field decreases the peak density.

Another interesting aspect of this calculation is the evolution of the electrostatic potential. Figure

3-18 shows the initial potential as having a dipole-like nature. The wind drag effect changes the potential behavior into a quadripole field because of the accumulation of wind drag related charge in the wake of the cloud. Figures 3-30 thru 3-34 illustrate the evolution of this quadripole field with time. Note that the magnitude of the peak potential associated with the wind drag wake grows continuously until by 425 seconds the wake potential has completely dominated the polarization potential of the ion cloud itself. This behavior agrees in principle with the mechanisms outlined in Section 2.3 although the magnitude of the wake potential may be somewhat surprising.

SECTION 4

CONCLUSIONS

In Section 2 it is shown through momentum conservation arguments that the reaction forces of ion clouds on the neutrals may be significant. This fact motivates the coupled ion-neutral flow calculations presented in Section 3. The results of the numerical calculation suggest that ion-neutral coupling effects may be a significant factor in the evolution of electrostatic plasma clouds. They suggest that morphological differences between small barium clouds, such as Avefria Dos, and large barium clouds, such as IRIS, ESTHER, and SPRUCE, could result from ion-neutral coupling effects.

In Section 2 a simple formula for the change in neutral wind velocity based upon a balance between momentum terms and ion drag terms is derived which indicates that ion drag effects could be significant in both large and small barium ion clouds. Section 2 also notes that viscosity can be an important parameter in the flow of the neutrals especially as the altitude increases because of the increases in kinematic viscosity. This observation is borne out by the numerical results of Section 3 which show that the neutral wind drag effect for the Avefria Dos cloud is controlled by viscous forces. Viscosity limits the decrease in neutral wind speed to 11 meters per second for this cloud where a 60 meter per second speed decrease might be expected from momentum considerations alone. An expression which accounts for both viscous and momentum terms to approximate the decrease in the neutral wind is presented in Section 3.2 and the

results of both the IRIS and the Avefria Dos flow calculations are found to be in reasonable agreement. The latter relation and the calculated results emphasize the importance of viscosity in high altitude neutral flow considerations.

The morphological difference which arises because of ion-neutral coupling effects is an initial increase in the ion cloud dimension perpendicular to the wind on the steepening side and then an eventual dimpling of this side. The dimpling is significant because it is the first such change in curvature of a contour noted in well-resolved unseeded numerical simulations.

Perhaps this type of coupling phenomenon might be responsible for the two-pronged fork appearance of PLACES event HOPE; although, it should be noted that the morphology resulting from ion-neutral coupling effects, as shown in Section 3.2 Figure 3-29 in particular, differs from the two-prong fork morphology of HOPE in that the angle of bifurcation is obtuse in the numerical results but acute in the HOPE data. Perhaps better agreement could be obtained from a three-dimensional analysis of the problem.

In Section 2.2 turbulence in the neutral wind is suggested as a possible source for structure. The scale size of expected eddy cells at lower altitudes are in close agreement with the structure sizes actually observed. Since few other physical mechanisms suggest the proper scale sizes of structure the neutral turbulence mechanism is viewed as a promising explanation. However, in light of the high viscosity of the higher altitude regions and its control on the neutral flow as

as observed in the Avefria Dos calculation of Section 3.2, it is probably the case that if turbulence is the cause of structure it must be localized in the E-layer coupling region.

Another consideration which must be made in considering neutral turbulence as a source of structure is the structure size. If structure were dependent upon turbulence in the near altitude vicinity of the barium plasma then higher altitude clouds should either not structure or have larger structures. A dependence of structure size upon altitude is not observed. However, on the other hand, if turbulence is created in the E-layer region it definitely will control the structuring of the barium cloud at higher altitudes and the sizes which arise will be more uniform and in closer agreement with observation. Key questions of this alternative explanation are is there pre-existing neutral turbulence in the E-layer and if there isn't can the image and image motion in this region produce neutral turbulence. The investigation of these questions is a topic for future efforts.

Clearly there are significant questions remaining concerning the role of ion-neutral coupling in the morphology and structuring of electrostatic ion clouds. These questions are highly relevant to late-time HANE plasma evolution because ion-neutral coupling should play a prominent role in their evolution. The purpose of this topical report is to open up avenues of thought into this interesting area of HANE late-time phenomenology.

REFERENCES

William F. Ames, Numerical Methods for Partial Differential Equations, San Francisco, Academic Press, 1977.

Sanborn C. Brown, Basic Data of Plasma Physics, Cambridge, MIT Press, 1959.

Warren C. Knapp and Kenneth Schwartz, Aids for the Study of Electromagnetic Blackout, General Electric-TEMPO, Defense Nuclear Agency Report DNA 3499H, February 1975.

Lewis M. Linson and David C. Baxter, Ion Cloud Modelling, Science Applications, Inc., Defense Nuclear Agency Final Report DNA 4455F, 1977.

Lewis M. Linson and Joseph B. Workman, "Formation of striations in ionospheric plasma clouds," J. Geophys. Res., Space Physics, 75, #16, June 1970, pp. 3211-3219.

Earl W. McDaniel, Collision Phenomena in Ionized Gases, New York, Wiley and Sons, 1964.

B.E. McDonald, M.J. Keskinen, S.L. Ossakow and S.T. Zalesak, Computer Simulation of Gradient Drift Instability Processes in Operation Avefria, Naval Research Laboratory, NRL Memorandum Report 4112, November 1979.

B.E. McDonald, S.L. Ossakow, S.T. Zalesak, and N.J. Zabusky, "Scale sizes and lifetimes of F-Region plasma cloud striations as determined by the condition of marginal stability," J. Geophys. Res., 86, July, 1981, pp. 5775-5784.

Robert C. Weast, ed. and Melvin J. Astle, assoc. ed., CRC Handbook of Chemistry and Physics, Boca Raton, Florida, CRC Press Inc., 1980.

DISTRIBUTION LIST

DEPARTMENT OF DEFENSE

Defense Nuclear Agency
ATTN: STNA
ATTN: NAFD
ATTN: RAEE
ATTN: NATD
ATTN: RAAE, P. Lunn
3 cy ATTN: RAAE
4 cy ATTN: TITL

Defense Tech Info Ctr
12 cy ATTN: DD

DEPARTMENT OF THE ARMY

BMD Advanced Technology Ctr
ATTN: ATC-T, M. Capps

Harry Diamond Labs
ATTN: DELHD-NW-P, 20240
ATTN: DELHD-NW-R, R. Williams, 22000

DEPARTMENT OF THE NAVY

Naval Ocean Systems Ctr
ATTN: Code 5322, M. Paulson
ATTN: Code 532
ATTN: Code 5323, J. Ferguson

Naval Rsch Lab
ATTN: Code 4720, J. Davis
ATTN: Code 4780
ATTN: Code 7500, B. Wald
ATTN: Code 4780, S. Ossakow
ATTN: Code 6700
ATTN: Code 7950, J. Goodman
ATTN: Code 4187
ATTN: Code 4700

Office of Naval Rsch
ATTN: Code 412, W. Condell
ATTN: Code 414, G. Joiner

Theater Nuclear Warfare Prj Office
ATTN: PM-23, D. Smith

DEPARTMENT OF THE AIR FORCE

Air Force Geophysics Lab
ATTN: OPR, H. Gardiner
ATTN: OPR-1
ATTN: LKB, K. Champion
ATTN: CA, A. Stair
ATTN: PHY, J. Buchau
ATTN: R. Babcock
ATTN: R. O'Neil

Air Force Weapons Lab
ATTN: SUL
ATTN: NTYC
ATTN: NTN

Air Force Wright Aeronautical Lab
ATTN: A. Johnson
ATTN: W. Hunt

Air University Library
ATTN: AUL-LSE

DEPARTMENT OF ENERGY CONTRACTORS

Los Alamos National Lab
ATTN: MS 664, J. Zinn
ATTN: P. Keaton
ATTN: D. Simons
ATTN: MS 670, J. Hopkins
ATTN: T. Kunkle, ESS-5
ATTN: R. Jeffries
ATTN: J. Wolcott
ATTN: C. Westervelt

Sandia National Lab
ATTN: D. Dahlgren
ATTN: Tech Library, 3141
ATTN: Space Project Div
ATTN: D. Thornbrough
ATTN: Org 1250, W. Brown
ATTN: Org 4231, T. Wright

DEPARTMENT OF DEFENSE CONTRACTORS

BDM Corp
ATTN: L. Jacobs
ATTN: T. Neighbors

Berkeley Rsch Associates, Inc
ATTN: J. Workman
ATTN: S. Brecht
4 cy ATTN: C. Prettie

EOS Technologies, Inc
ATTN: B. Gabbard

ESL, Inc
ATTN: R. Ibaraki
ATTN: R. Heckman
ATTN: J. Lehman
ATTN: E. Tsui
ATTN: J. Marshall

Honeywell, Inc
ATTN: G. Collyer, Avionics Dept
ATTN: G. Terry, Avionics Dept

Institute for Defense Analysis
ATTN: E. Bauer

JAYCOR
ATTN: J. Sperling

Kaman Tempo
ATTN: B. Gambill
ATTN: DASIAC
ATTN: J. Devaney
ATTN: W. Knapp
ATTN: K. Schwartz
ATTN: W. McNamara

Pacific-Sierra Rsch Corp
ATTN: H. Brode, Chairman SAGE

Physical Dynamics, Inc
ATTN: E. Fremouw

DEPARTMENT OF DEFENSE CONTRACTORS (Continued)

Mission Research Corp
ATTN: R. Hendrick
ATTN: C. Lauer
ATTN: R. Kilb
ATTN: F. Fajen
ATTN: R. Bigoni
ATTN: G. McCartor
ATTN: F. Guigliano
ATTN: Tech Library
ATTN: S. Gutsche
ATTN: R. Bogusch

R & D Associates
ATTN: R. Lelevier
ATTN: C. Greifinger
ATTN: R. Turco
ATTN: H. Ory
ATTN: W. Wright
ATTN: M. Gantsweg
ATTN: W. Karzas
ATTN: F. Gilmore

R & D Associates
ATTN: B. Yoon

Rand Corp
ATTN: E. Bedrozian
ATTN: C. Crain

DEPARTMENT OF DEFENSE CONTRACTORS (Continued)

SRI International
ATTN: G. Price
ATTN: R. Tsunoda
ATTN: J. Vichrey
ATTN: W. Chesnut
ATTN: R. Livingston
ATTN: D. Neilson
ATTN: J. Petrickes
ATTN: O. McDaniels
ATTN: R. Leadabrand
ATTN: M. Baron
ATTN: A. Burns
ATTN: C. Rino
ATTN: G. Smith
ATTN: V. Gonzales
ATTN: W. Jaye

VisiDyne, Inc
ATTN: C. Humphrey
ATTN: O. Shepard
ATTN: W. Reidy
ATTN: J. Carpenter

Science Applications, Inc
ATTN: L. Linson
ATTN: C. Smith
ATTN: E. Straker
ATTN: D. Hamlin


ATE
LME